Bettina Höfer BSc

Simplifying NMR Spectra by interrupted Acquisition Methods

MASTERARBEIT

zur Erlangung des akademischen Grades

Master of Science

Masterstudium Chemie

eingereicht an der

Technischen Universität Graz

Betreuer

Ao.Univ.-Prof. Mag. Dr.rer.nat. Klaus Zangger

Institut für Chemie

Karl-Franzens-Universität Graz

Graz, Mai 2016

EIDESSTATTLICHE ERKLÄRUNG

Ich erkläre an Eides statt, dass ich die vorliegende Arbeit selbstständig verfasst, andere als die angegebenen Quellen/Hilfsmittel nicht benutzt, und die den benutzten Quellen wörtlich und inhaltlich entnommenen Stellen als solche kenntlich gemacht habe. Das in TUGRAZonline hochgeladene Textdokument ist mit der vorliegenden Masterarbeit identisch.

Datum

Unterschrift

"DON'T PANIC!"

The Hitchhiker's Guide to the Galaxy by Douglas Adams

Danksagung

An dieser Stelle möchte ich allen Menschen danken, die mir während meines Studiums geholfen und mich motiviert haben.

Ganz besonderer Dank gilt Prof. Klaus Zangger, der mir mit hilfreichen Anregungen und konstruktiver Kritik sowohl bei meiner praktischen Arbeit als auch beim Verfassen dieser Masterarbeit zur Seite stand.
Außerdem möchte ich mich bei der ganzen Arbeitsgruppe Bio-NMR bedanken, dass ich jederzeit mit Fragen zu euch kommen durfte und ihr mir so viele Arbeitstechniken beigebracht habt.

Ich danke vor allem meinen Eltern für jegliche Unterstützung, die ich während meiner Studienzeit von euch erfahren habe. Ihr habt mir immer zugehört, wenn ich etwas auf dem Herzen hatte, und habt mich ermutigt, weil ihr immer an mich geglaubt habt. Danke auch an meinen Freund, der hinter mir stand und mir stets Mut zusprach.

Zuletzt möchte ich mich bei meinen Freunden und meinen genialen Studienkollegen bedanken, denn ohne unsere gemeinsamen Lerntreffen, Gruppenarbeiten und das gelegentliche Prüfungsbier wäre der Weg zum Abschluss viel beschwerlicher gewesen!

Kurzfassung

NMR-Spektroskopie ist eine mächtige Methode zur Strukturaufklärung. In dieser Masterarbeit werden Ergebnisse von Forschung an zwei Themen präsentiert.
Pure shift NMR wird zur homonuklearen Breitbandentkopplung angewendet um Auflösung in protonen-detektierten Spektren zu gewinnen. Slice-selektives (Zangger-Sterk) Entkoppeln scheint die Kopplung von stark gekoppelten Spins zu entfernen, so dass die beteiligten Signale zu einem Signal zusammenfallen. Deshalb wurden Parameter der Zangger-Sterk-Entkopplungsmethode (chunking time, Pulslänge des selektiven 180° Pulses und die Dauer des Delays vor und nach dem selektiven Puls) verändert und angepasst um ein Signal aus den beiden stark koppelnden Spins zu erzeugen. Ein Singulett bildet sich, wenn die Zeit des Chunks zwischen 10 und 15 ms liegt. Allgemein wurde gefunden, dass ein kurzer Puls und ein langes Delay die schärfsten Signale erzeugen. Wenn die J-upscaling Sequenz verwendet wurde, konnten die Signale verschmolzen werden, allerdings spalteten sie sich wieder auf, wenn der gewählte J-Faktor zu hoch war. Simulationen mit SIMPSON wurden ausgeführt um den Einfluss von steigender skalarer Kopplung und abnehmender Differenz der chemischen Verschiebung auf die Anzahl der Signale und ihrer Intensität im Spektrum zu zeigen.
Als Anwendungsbeispiel von homonuklearer Breitbandentkopplung wollte ich diesen Ansatz an Lipopolysacchariden der Bakterien *Escherichia coli BL21(DE3)* und *Escherichia coli Nissle 1917* verwenden. Im zweiten Teil meiner Masterarbeit wurden die Extraktion und weitere Aufreinigung der Lipopolysaccharide von *E.coli Nissle 1917* etabliert um eine weitere Charakterisierung mittels pure shift NMR zu ermöglichen.

Abstract

NMR spectroscopy is a powerful tool for structure determination. In this master thesis research on two connected topics is presented.

Pure shift NMR is used for broadband homonuclear decoupling in order to gain resolution in proton-detected spectra. By using slice-selective (Zangger-Sterk) decoupling of strongly coupled spins seems to remove strong coupling by collapsing the involved signals. Therefore parameters of the Zangger-Sterk method (chunking time, pulse width of the soft 180° pulse and the delay before and after this pulse) have been adjusted to generate one signal out of two decoupled spins. A singlet can be generated using a proper chunking time, which turned out to be between 10 and 15 ms. Generally a short pulse and long delay give the sharpest peaks. Signals could be merged into a singlet using J-upscaling but disappeared when the upscaling factor was too high. Simulations with SIMPSON showed the impact of increasing scalar coupling and decreasing chemical shift difference on the number of signals and their signal intensity in a spectrum.

As a test case for homonuclear broadband decoupling I wanted to use this approach on lipopolysaccharides of *Escherichia coli BL21(DE3)* and *Escherichia coli Nissle 1917*. In the second part of my thesis I established the extraction and purification of lipopolysaccharide from *E. coli Nissle 1917* for further characterization by pure shift NMR.

Content

1 Aim of this work

Nuclear magnetic resonance is a powerful tool for structure determination and finds special application in structural biology. Biological molecules (e.g. proteins or lipopolysaccharides) are dissolved in buffered deuterated solvents before measurement; hence it is possible to simulate their biological environment. This capability gives NMR a big advantage over the widely used crystallography.Although many methods have been invented to gain as much structural information as possible, resolution is still an issue. A very successful approach to simplify crowded spectra is the Zangger-Sterkmethod.[1]By using gradients and a combination of hard and soft 180° pulses, protons are decoupled from each other; instead of a complicated multiplet, a singlet will occur in a decoupled spectrum.

This master thesis has several aims.

Homonuclear decoupling using slice-selective excitation is a universal technique, which is applicable for every type of molecule. Admittedly strongly coupled signals give some trouble, because they change drastically with certain parameters and usually give strong artefacts. The ZS-pulse sequence is used to determine how strongly coupled signals can be influenced and simulations are performed to create a method, which is able to collapse strongly coupled signals into one singlet ultimately.

In order to find an application for slice-selective homonuclear decoupling, we targeted lipopolysaccharides. These molecules build the outer cell wall of gram-negative bacteria. Until now they needed to be extracted for NMR measurements. Our goal is to record spectra of living cells, where it is possible to determine their structure. To get a reference substance, lipopolysaccharides need to be extracted and so an extraction protocol was established.

2 Strong coupling

2.1 Introduction

Proton-proton coupling can make spectra very crowded, therefore a big effort has been made to invent decoupling sequences. One of these methods is the slice-selective decoupling, also known as Zangger-Sterk method. When applying the Zangger-Sterk (ZS) method for decoupling, strongly coupled signals give strange effects. Therefore strong coupling was investigated.

2.1.1 Strong coupling

Two spins, which are scalar coupled, give a doublet at each of the two offsets. The two signals of one doublet have the same distance in Hertz, which we call scalar coupling J. The lamor frequency at which one spin processes is calculated:[2]

$$v_{0,1} = -\frac{1}{2\pi}\gamma_1(1+\delta_1)B_0$$

Equation 1lamor frequency is calculated from its offset, gyromagnetic ratio and the magnetic field

$v_{0,1}$& $v_{0,2}$	larmor frequencies of spins 1 and 2
γ_1&γ_2	gyromagnetic ratios
δ_1&δ_2	shifts of spins 1 and 2
B_0	magnetic field

For weakly coupled spins, the positions of signals can be estimated, when lamor frequencies and the coupling factor J is known.

Table 1 positions of two doublets in a spectrum

Signal	Position in the spectrum
A	$v_1 + 0{,}5\ J_{12}$
B	$v_1 - 0{,}5\ J_{12}$
C	$v_2 + 0{,}5\ J_{12}$
D	$v_2 - 0{,}5\ J_{12}$

In a spectrum of two coupled spins we see two doublets, these four signals resemble the transitions between spin states occur at certain frequencies. All signals of the two doublets have the same intensity.

When we look at two weakly coupled homonuclear spins, like two protons, their lamor frequencies are very similar and in the range of MHz, while their coupling constant is in Hz.
A spin system is strongly coupled when the difference of lamor frequencies is very small compared to their scalar coupling. Therefore strong coupling rather occurs in spectra recorded at lower frequencies, but even at higher frequencies strong coupling can occur.[3]
To evaluate how strong a coupling is, a strong coupling parameter ξ can be calculated.
ξ is an angle, which is determined by:[2]

$$\tan(\xi) = \frac{J_{12}}{v_{0,1} - v_{0,2}}$$

Equation 2 the strong coupling factor ξ can be estimated from the coupling constant and the chemical shift difference of two spins

Two strongly coupled spins can have four energy levels, each defined by one eigenfunction. two of those eigenfunctions are the same as for weakly coupled spins, the other two are combinations of weakly coupled eigenfunctions and are dependent on the strong coupling parameter ξ. When no strong coupling is present, ξ is zero and hence the sinus-term becomes zero and the energy level is defined only by one wave function.
In a spectrum, strongly coupled spins can be recognized by the roofing effect, where for example the outer signals of two doublets have smaller intensities than the inner ones. This intensity effect can again be calculated with the strong coupling parameter. The stronger the coupling is, the smaller the outer signals become.

Table 2 Signal intensity of strongly coupled signals is dependent on the strong coupling factorξ

Transition/ signals	Frequency	Intensity
A	$+\frac{1}{2}D - \frac{1}{2}\Sigma - \frac{1}{2}J_{AB}$	$\frac{1}{2}(1 + sin\xi)$
B	$+\frac{1}{2}D - \frac{1}{2}\Sigma + \frac{1}{2}J_{AB}$	$\frac{1}{2}(1 - sin\xi)$
C	$-\frac{1}{2}D - \frac{1}{2}\Sigma - \frac{1}{2}J_{AB}$	$\frac{1}{2}(1 - sin\xi)$
D	$+\frac{1}{2}D - \frac{1}{2}\Sigma + \frac{1}{2}J_{AB}$	$\frac{1}{2}(1 + sin\xi)$

Not only intensities but also the chemical shift is different in strongly coupled systems. Usually two signals of a doublet are centered around the chemical shift symmetrically; hence the chemical shift can be extracted from a spectrum easily. When strong coupling is present, the outer signal moves away from chemical shift and the inner signal is positioned closer at the chemical shift. Interestingly, the distance between two signals of a doublet is always the scalar coupling constant. The outcome of this is, that the scalar coupling constant J can be

extracted easily from weakly and strongly coupled spectra, but the chemical shift of strongly coupled spins have to be calculated.

$$D = \sqrt{\left(v_{0,1} - v_{0,2}\right)^2 + J_{AB}^2}$$

$$\Sigma = v_{0,1} + v_{0,2}$$

Equation 3 D and E are determined by J-factor and lamor frequencies

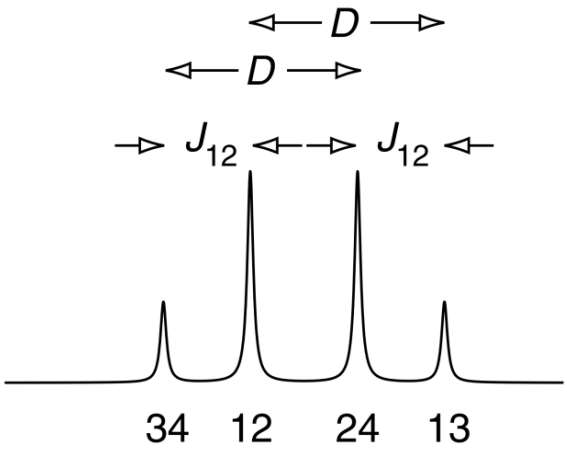

Figure 1 Two strongly coupled doublets and factor D and J explained; figure from[2]

Looking at spectra of two strongly coupled spins, we can see the intensities of the outer signals diminishing with increased coupling. When the lamor frequencies of two spins become the same (v1=v2), ξ becomes 90° and only one signal is present.

2.1.2 Decoupling

In order to gain resolution in a proton spectrum, it is beneficial to convert multiplets into singlets.[4] Various decoupling techniques have been published, one of the most successful ones is slice-selective decoupling.[5]

The principle is similar to band-selective decoupling. All spins are excited by a 90° pulse, after a time τ they get rotated by a 180° hardpulse. Only a certain frequency gets rotated back by a 180° selective pulse. After a second time τ, some spins have experienced a zero net rotation while the others are rotated by 180°.

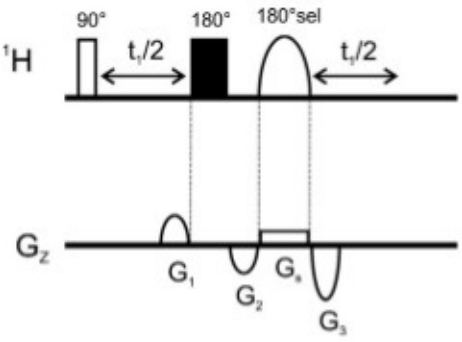

Figure 2 The Zangger-Sterk method; Figure taken from[5]

This pulse sequence would give a band-selective decoupled spectrum. It is implemented in several other pulse sequences.[6] To gain a broadband decoupled spectrum, a gradient in z direction is applied. Because of this gradient the magnetic field at each location of an NMR tube is slightly different, dividing it into slices. When a selective pulse is applied simultaneously with the gradient, different frequencies, which are on resonance in a particular slice, get excited. Using this method every signal of a spectrum can be decoupled.
Because the decoupled signal is arising just from one excited slice, the overall intensity of a slice-selective decoupled spectrum is much lower than from a normal proton spectrum.
We investigated homonuclear decoupling of strong couplings using this slice-selective decoupling method.[7] The FID arising from this pulse program is not recorded in one piece, but in small "data chunks". Between those data chunks a pair of a selective and non-selective 180° pulse is applied.[7] This pulse sequence has been improved by variation of the length of data chunks, so eventual decoupling artefacts are averaged out.[8]

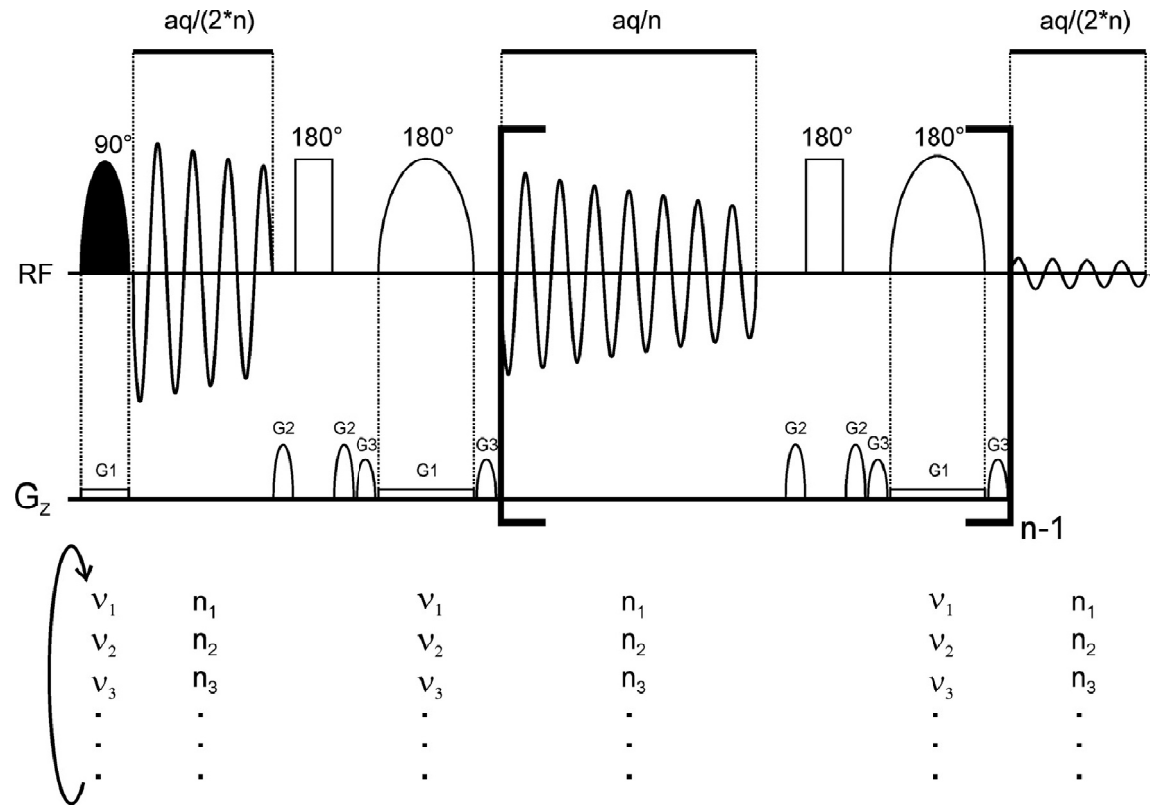

Figure 3 Slice selective decoupling sequence, the length of data chunks is varied by a variable loop delay; figure from [8]

2.1.3 J-Upscaling

Scalar coupling provides a lot of information, which can be used for structural interpretation. The scalar coupling can be easily measured from the distance of two lines from a multiplet. But some couplings may not be resolved because they are too small or signals are too broad. A method to enhance scalar coupling has been published recently by Glanzer et al.

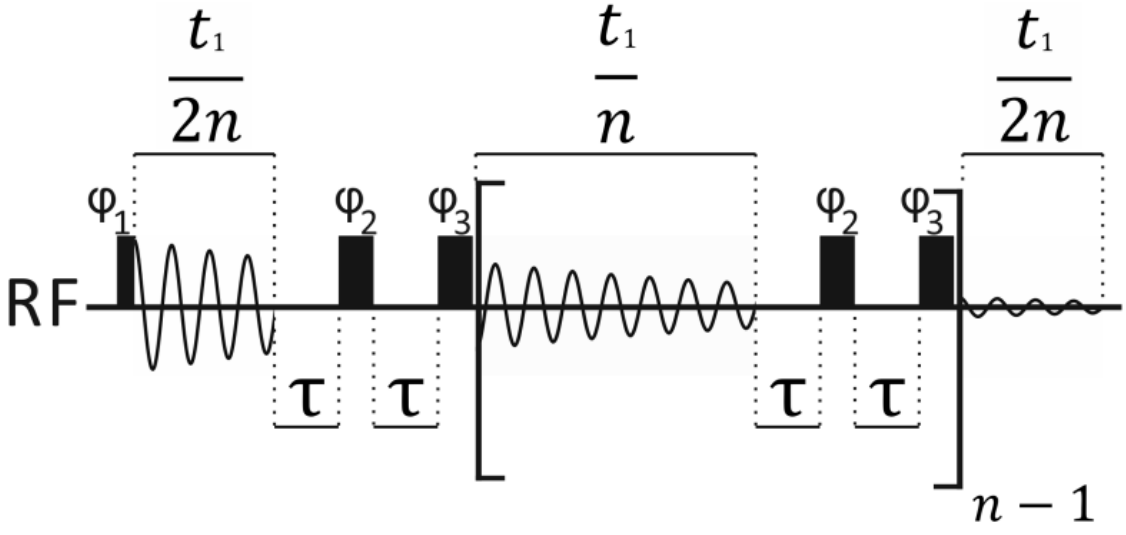

Figure 4 Pulse sequence for J-upscaling; Figure from [9]

The principle of a J-upscaling sequence is to refocus chemical shift while scalar coupling is allowed to evolve. During acquisition scalar coupling and chemical shift evolve, a 180° hard pulse refocuses the chemical shift but does not affect scalar coupling, a second 180° hard pulse rotates the chemical shift back and another data acquisition chunk starts.
Since scalar coupling is allowed to evolve, but chemical shift evolution is suppressed, scalar coupling is enhanced by a factor depending on delay time τ and data acquisition time t_1.
The effects of the J-upscaling NMR experiment were investigated on strong coupling signals.[9]

2.2 Methods

All experiments were measured on a 500MHz BrukerAvance III NMR spectrometer .
Fumaric acid, aspartic acid and asparagine were purchased from Sigma Aldrich.Deuterated solvents D_2O, DMSO-d_6 and $CDCl_3$ were obtained from Eurisotop

2.2.1 ZSDecoupling

For this experiment, the 90° selective pulse was an Eburp2.1000 pulse and the 180° selective pulse was a Gauß1_180r.1000. At first, the pulse width of a 180° selective pulse (p13) was varied in order to achieve "superdecoupling" - a single signal of 2 collapsed strong coupling partners. Further the delay d7, which is placed right before and after the Gauß-pulse was varied. At last the number of loops was modified and a variable loop counter, which suppresses decoupling-artefacts, was applied.

2.2.2 J-upscaling

Since we wanted to increase strong coupling so far as to collapse two signals, Glanzer and Zangger's J-upscaling method was employed. The behaviour of strongly coupled signals was observed by enhancing scalar coupling up to a factor of 4. J-upscaling is recorded in data chunks, so the chunking-time, which is the acquisition time of one block, was varied. Additionally all 180° hard pulses were substituted by two 180° pulses, giving 4 pulses in one acquisition block instead of 2.

2.2.3 Simulations with Simpson[10–12]

Simple spectra of two doublets of coupled spins were simulated with Simpson and viewed with Simplot. Simpson is a simulation program for solid state NMR but with little changes in the code, liquid state NMR systems can be simulated too. The system investigated was composed of two spins, which are coupling to each other and therefore give two doublets. The effect of different coupling-constants on those signals was investigated.

2.3 Results and Discussion

2.3.1 ZS Decoupling

Aspartic acid has two protons at 2,94 ppm coupling to a -CH group and to one another, each giving two doublets. The coupling between those protons is 18,21 Hz. By screening various pulse widths of the Gaußpulse, we found out that a pulse width of 10 ms was sufficient to create a singlet in the decoupled spectrum. The delay d7 was 3 ms and the spectrum was recorded with 60 loops, giving a chunking time of 0,0273 s. Artefacts were present, so a variable loopcounter was integrated in the pulse sequence. A loop number of 8, giving a chunking time of 0,02048 s, proved to be right. Pulse width and delay time (d7) were varied so that the sum of both would give 10 ms. The best result was achieved with d7=3 ms and p13 =4 ms.

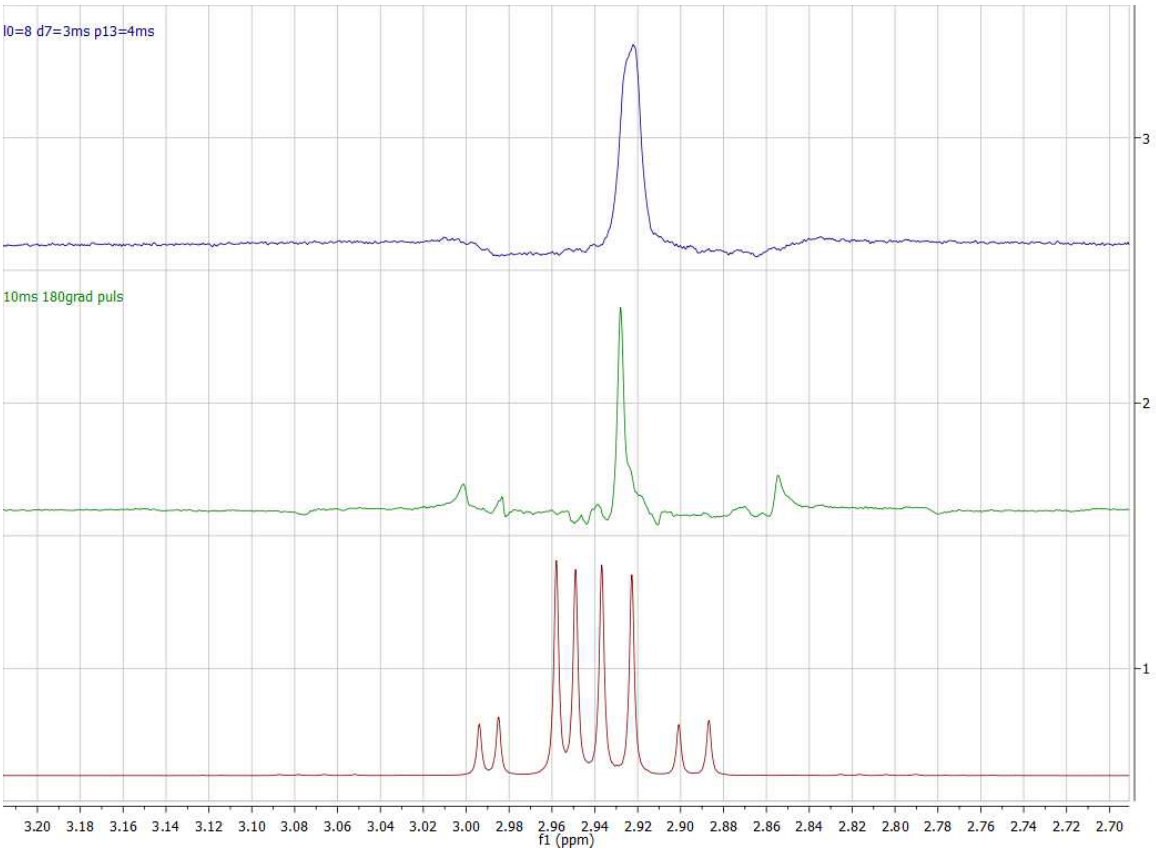

Figure 5 1H spectrum of aspartic acid, a ZS-decoupled spectrum without variable loop counter and a ZS-decoupled spectrum with a variable loop counter

Two protons of asparagine at 2,85 ppm are strongly coupled. Both show a double-doublet as coupling pattern. Their J-coupling with 17,19 Hz is smaller than the J-constant of aspartic acid. Using the ZS-decoupling sequence without variable loop counter, we found the best results when employing 110 loops, a delay d7 of 7,5 ms and a pulse width for the Gauß-pulse of 4 ms. This sums up to 15 ms. Unfortunately the decoupling artefacts were very strong, so an experiment with variable loopcounter was made. As for aspartic acid we found L0=8 (chunking time 0,02048 s) to be sufficient. Pulse width and delay d7 were varied, but always gave a sum of 15 ms. A single signal was measured with a setup of L0=8, d=7,5 ms and p13=4 ms. The variable loop counter improved the spectrum, but artefacts are still visible. The arising signal looks decoupled but one can see that the signal is not properly formed and the top is somehow cut.

This might be the case because the J-constant is about 1 Hz smaller than the one from Asp. Therefore the coupling itself is smaller and the signals are not so very much strongly coupled as the ones from Asp.

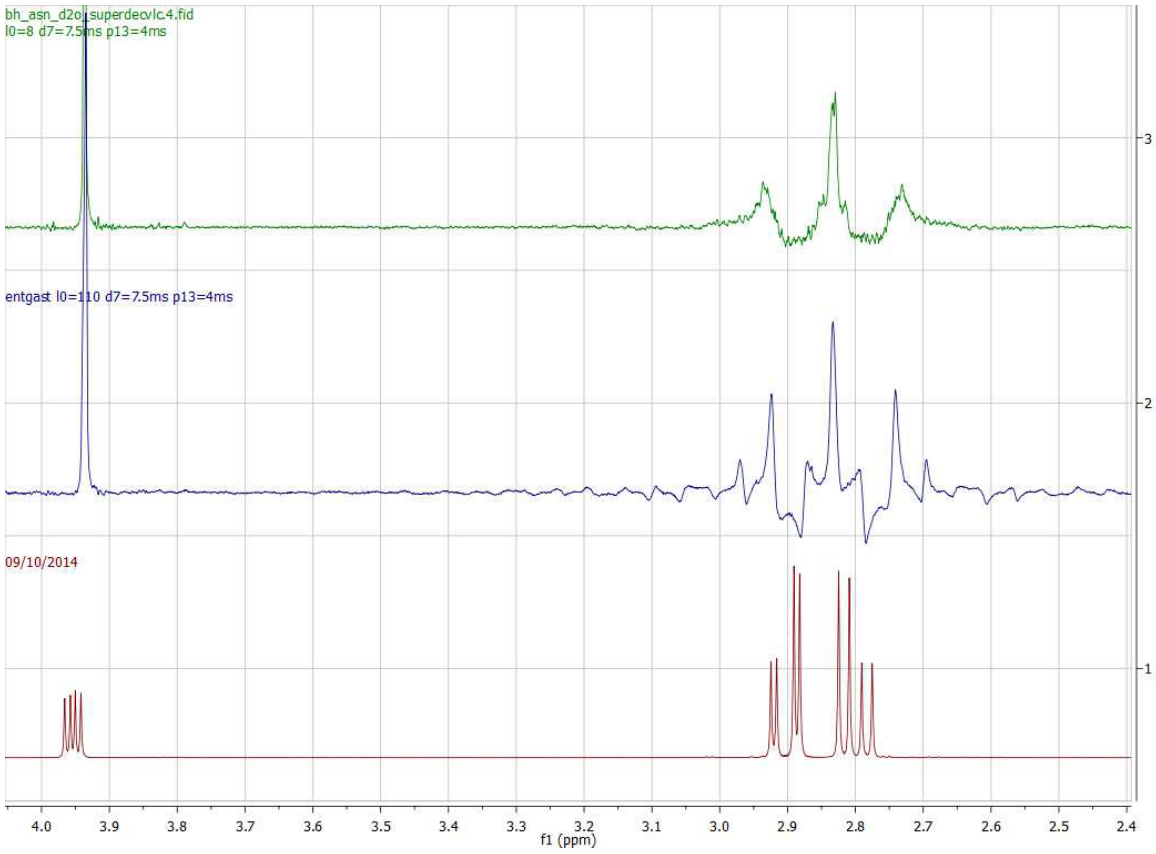

Figure 6 1H spectrum of asparagine, two decoupled spectra one without VLC, the top one with VLC

Fumaric acid possesses two strongly coupled protons, which are attached to different carbons. Those carbons are bound through a double bond. They only couple to each other, so two doublets are found in a spectrum.

To decouple the signals, a pulse width of 1 ms for the p13-pulse and a d7-delay of 7 ms was sufficient. Again the sum of this block is 15 ms and different combination of pulse widths and delays were tried out. Despite the fact that mainly one signal was present even for completely different parameters, like d7=2,5 ms and p13=10 ms, we could see that the signal, which was recorded with d7=7 ms and p13= 1ms, gave the sharpest peak.

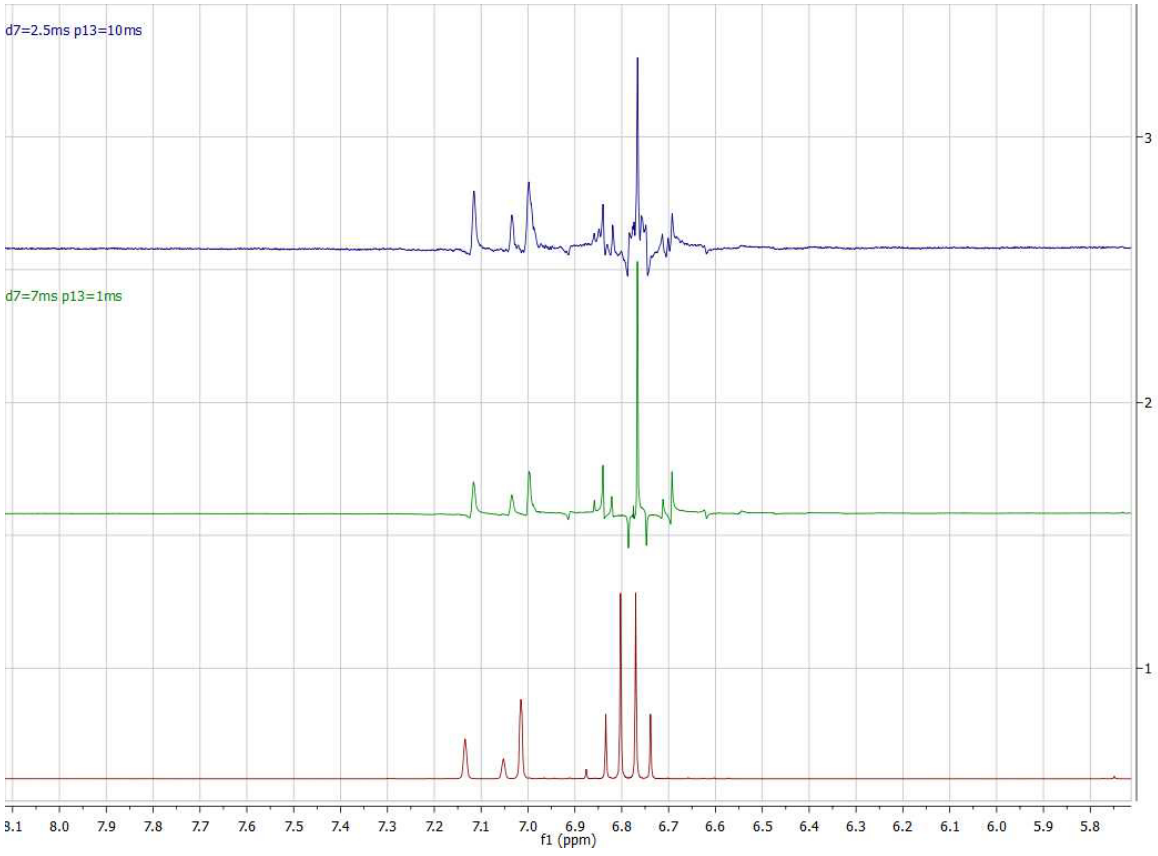

Figure 7 Regular ^{1}H spectrum of fumaric acid, two decoupled spectra; pulse width and delays sum up to 15 ms for both spectra

All in all, it looks like the sum of pulse width and delay time have a certain value for certain coupling. Sharp signals can be achieved when the delay time is long but the pulse short and powerful.

2.3.2 J-upscaling

Fumaric acid is an appropriate substance for investigating strong coupling, because the coupling protons are not bound to the same carbon and they are only coupling with each other, so they only give two doublets. Two doublets are the easiest case of strong coupling. Several spectra of fumaric acid were measured with the goal of collapsing the signals of two spins.

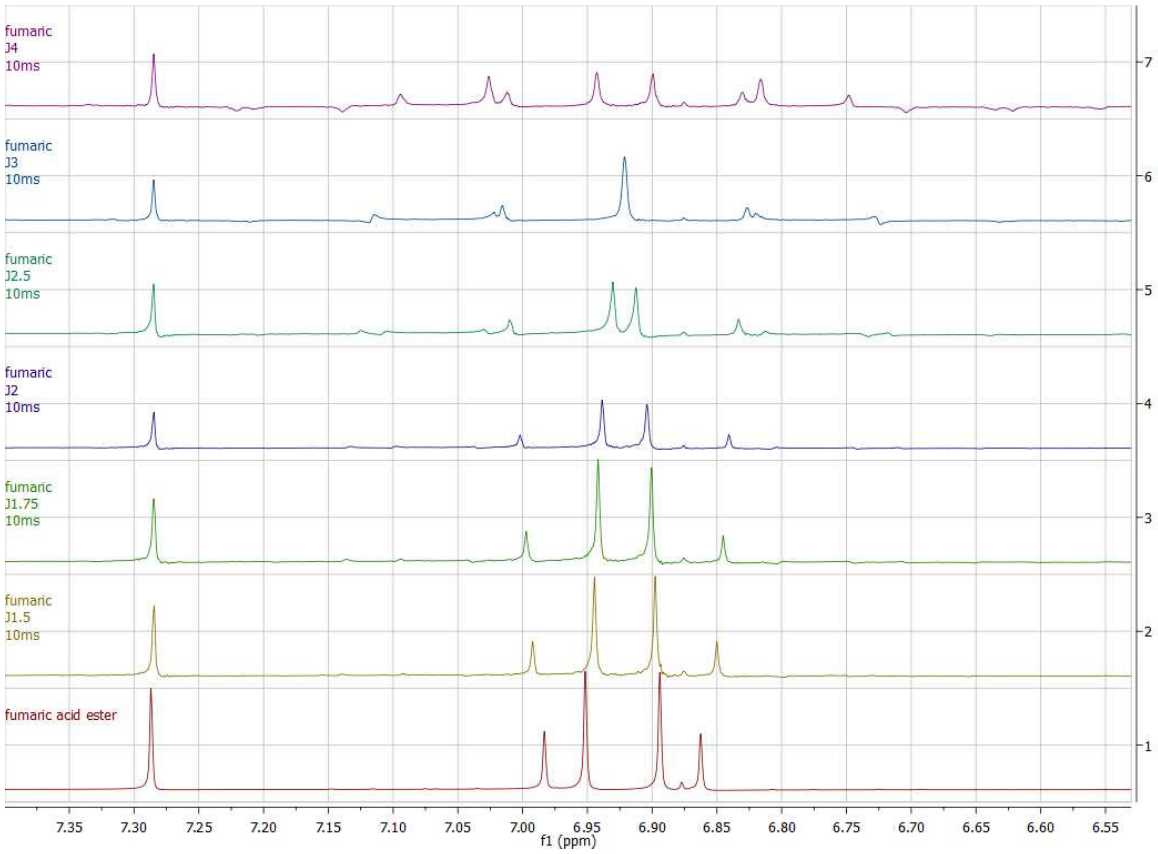

Figure 8 J-upscaling spectra of fumaric acid; J:0; J:1,5; J:1,75; J:2; J:2,5; J:3; J:4

As can be seen above, the scalar coupling of the two protons can be enhanced, the outer signals become smaller and smaller, while the inner signals come closer together. For a chunking time of 10 ms, a J-scaling factor of 3 creates what seems to be one signal with very small signals nearby. But when a scaling factor of 4 is applied, the two "inner" signals move past each other because their coupling constant is so big.

This result is not surprising, since we know that J-upscaling is not really increasing the coupling itself, but it is only reducing chemical shift evolution. From theory we know that only when the chemical shift is exactly the same, we will see a singlet in a regular proton spectrum. What we can derive is, that once a singlet is created because of coupling-enlargement, it should stay a singlet when the J-coupling becomes even larger.

2.3.3 SIMPSON

A system of 2 spins coupling to each other was simulated. First, a constant coupling of 50 Hz was applied and the chemical shift difference was decreased.

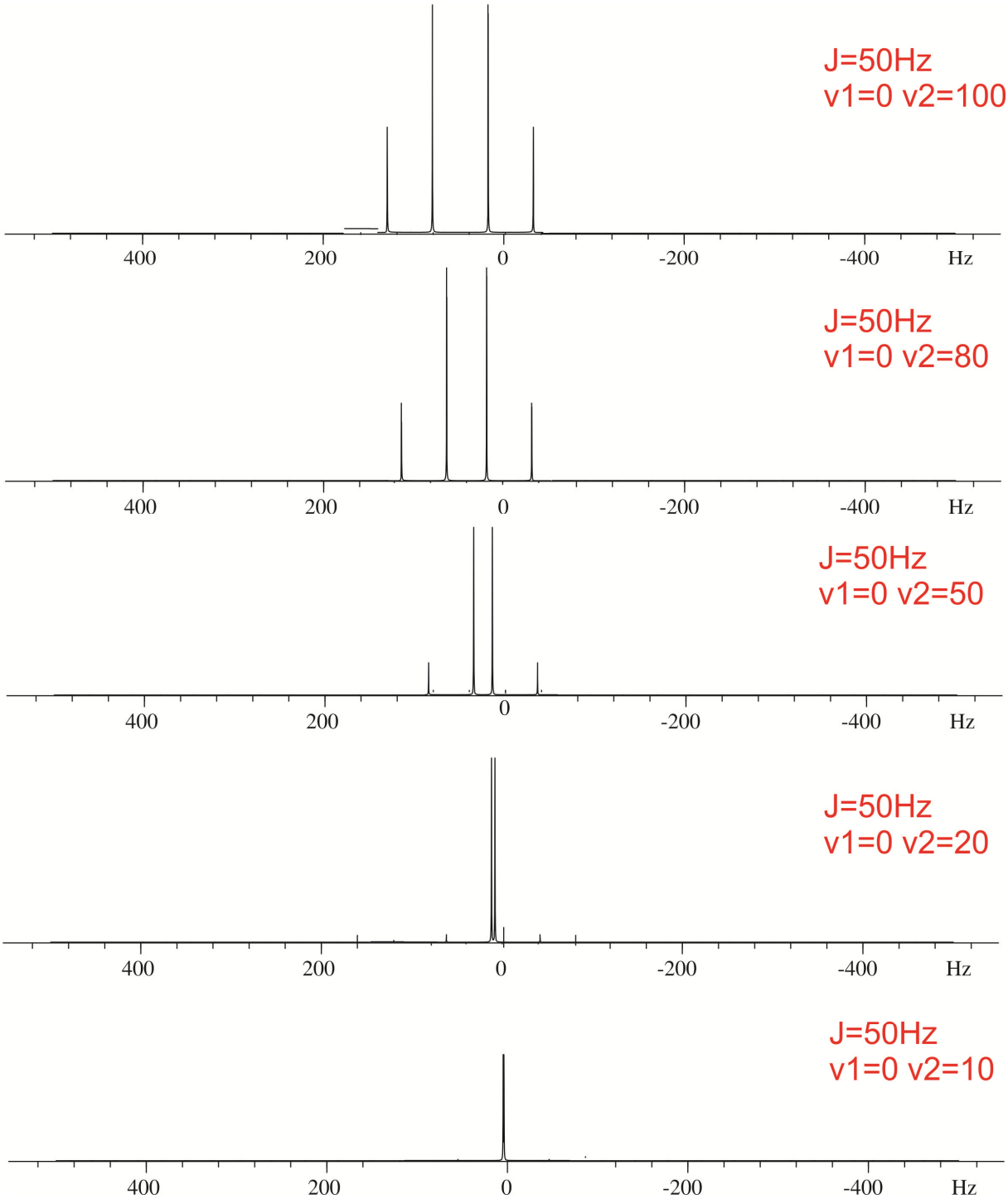

Figure 9Simpson simulation of two spins with a scalar coupling of 100 Hz and decreasing chemical shift differences

It can be seen clearly that with smaller chemical shift difference, the intensity of outer signals decreases. The second doublet is asymmetrically centeredaround 0 Hz. When the difference

is 20 Hz, the outer signals become so small that they are not visible anymore. Because of an implemented line broadening function, a single signal is created when the chemical shift difference is 1/5 of the coupling constant.

In another simulation the chemical shift difference was left at constant 100 Hz and the scalar coupling was increased. When there is no coupling present, two singlets appear in the spectrum. The bigger the coupling becomes, the smaller the intensity of the outer signals. Even with a coupling constant, which is 5 times bigger than chemical shift difference, it is not possible to collapse the doublets completely.

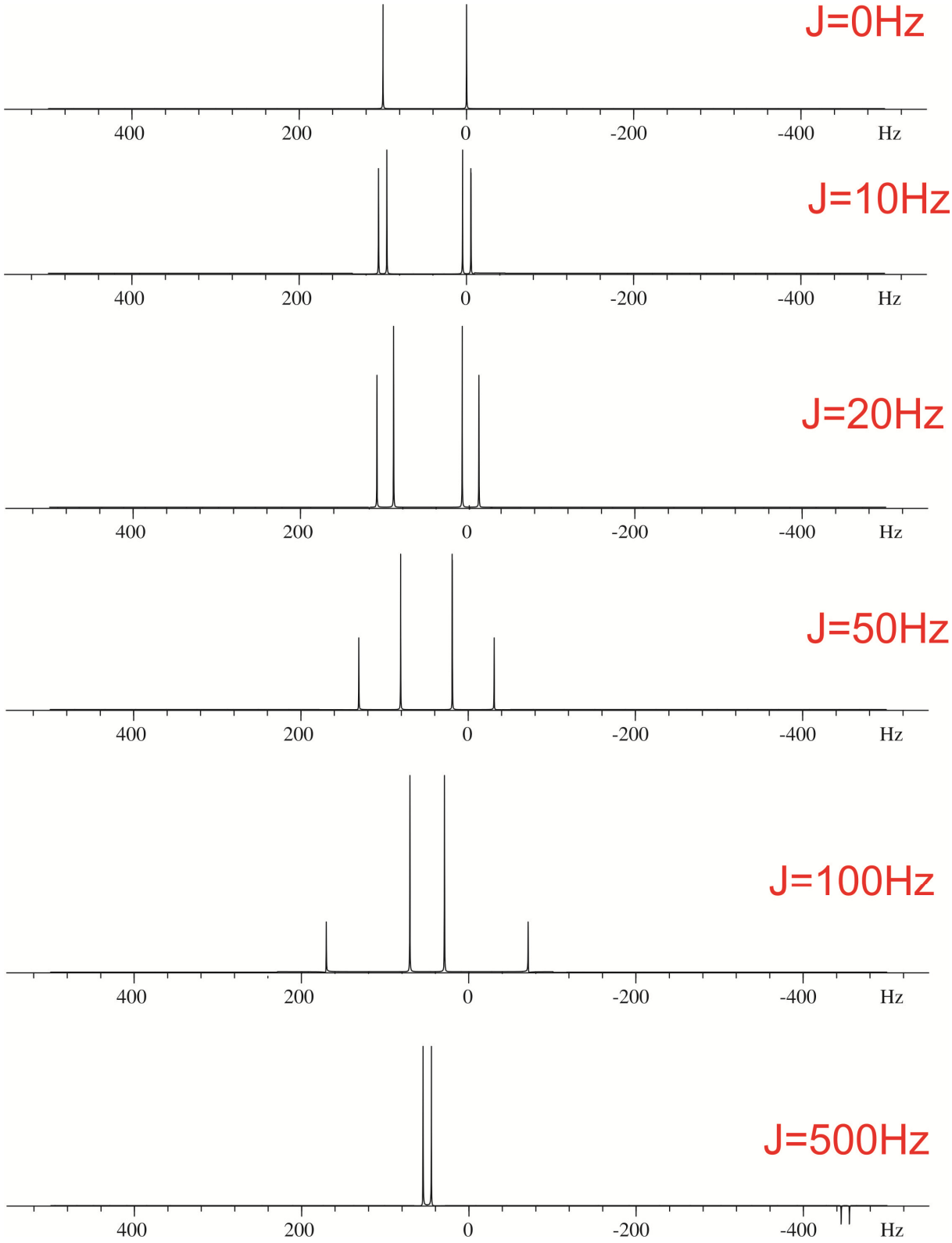

Figure 10 Simpson simulation of two spins with a chemical shift difference of 100 Hz and increased scalar coupling

2.4 Conclusion

We successfully decoupled strongly coupled signals and generated one signal using slice-selective decoupling. But we could not find general parameter-settings. We tried to collapse signals using J-upscaling but proved that scalar coupling itself is not increased with this pulse sequence. Simulated spectra of a spin-echo experiment were generated with SIMPSON, but it was not possible to simulate data chunking. In order to really understand how strong coupling is affected by decoupling and especially data chunking, it is necessary to simulate this pulse sequence too and calculate the density matrix of the spin system after data chunking. This will give insight to the effects of decoupling on strongly coupled spins.

3 Lipopolysaccharide extraction

3.1 Introduction

A gram-negative cell is composed of up to 10^6 lipopolysaccharide-residues, which are located on the outer cell wall.[13] Several methods of extraction and further purification were applied to gain very pure lipopolysaccharides for NMR measurements.

3.1.1 Lipopolysaccharide

Cell walls of gram-negative bacteria consist of two membranes, the cytoplasmic and the outer membrane, which are separated by the periplasmic space.[14] A bilayer of phospholipids makes up the cytoplasmic membrane. The outer membranes building block is again a phospolipidbilayer but also porines, lipoproteins and lipopolysaccharides are present.[15]

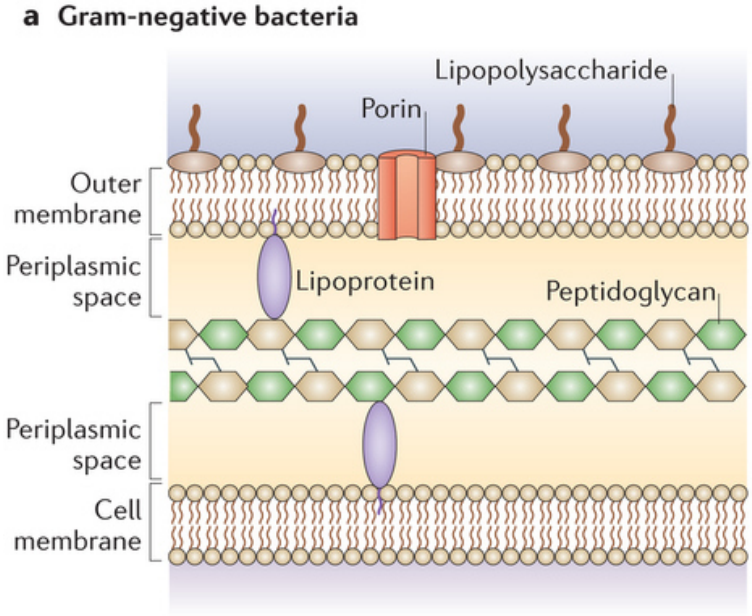

Figure 11 The outer cell wall of gram negative bacteria consists of an inner and an outer cell membrane; LPS are anchored at the outer cell membrane; picture from [14]

The lipid part of lipopolysaccharides is anchored on the outer side of the membrane, so that the polysaccharide is the outermost part of a gram-negative cell. Lipopolysaccharide transport proteins export the LPS from the inner cell membrane to the outside of the outer membrane.[16][17]

Lipopolysaccharides consist of three distinctive parts: Lipid A, a core oligosaccharide and an O-antigen. The exact composition of an LPS varies from species to species, but the main parts gave always the same general structure.[15] When all three components are present it is

referred to as smooth type lipopolysaccharide. If there is a lack of O-antigen the lipopolysaccharide is called "rough".

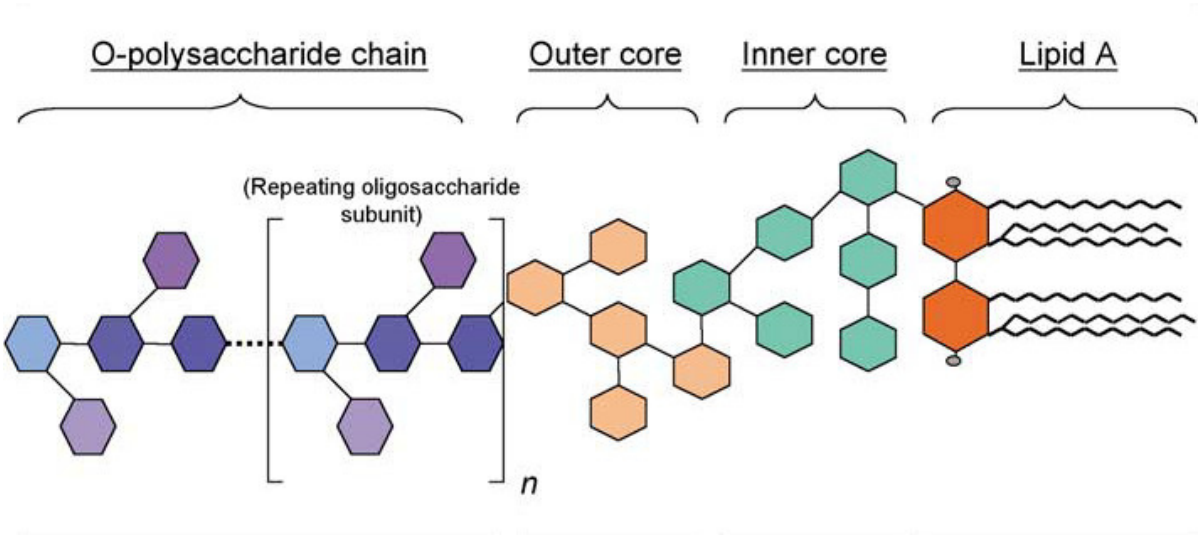

Figure 12 Structure of lipopolysaccharides from C. Erridge et al.[18]

Lipid A is a glucosamine disaccharide, which is phosphorylated at positions 1 and 4' and has fatty acids linked to it by ester- or amide-bonds.[18] In *Escherichia coli* Lipid A consists of six fatty acids, but also structures with five or less fatty acids like the ones of *Bortella pertussis* and *Chlamydia trachomatis* are known.[19] The attached fatty acids are in most cases saturated and their length can vary with species. *E.coli* has five C_{14} fatty acid moieties and one C_{12} moiety.

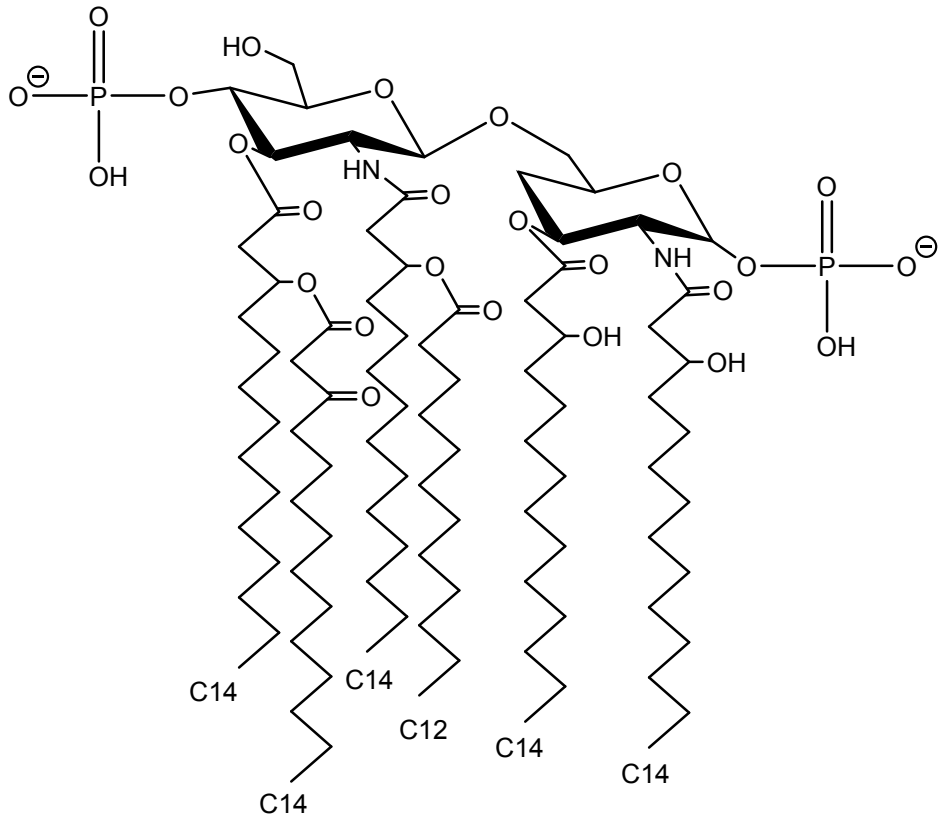

Figure 13Structure of *E.coli* Lipid A[13]

Whereas Lipid A is highly conserved within a species, and the o-antigen is specific for one strain, there can be found several core oligosaccharide structures in a species. In *E.coli* five core structures(R1-R4, K-12) are found. The core oligosaccharide can be further divided into the inner and the outer core. The inner core is directly attached to the Lipid A and consists of 8-12 [19] unusual sugars like KDO and heptose.[18] Particularly KDO is very important, because it is proven that the smallest LPS existing consists of one KDO, which is alpha-bound to Lipid A. This KDO also has a substituent, typically phosphate on it.

The outer core consists of up to 6 rather usual sugars like glucose and galactose.

The five core structures occurring for *E.coli* have a similar inner core region but differ in the outer core structure. All of them are have a backbone made out of three hexose-sugars and they have two side chains. Core R1's backbone consists of one Gal, two Glc and one Hep and has a Gal and Glc attached at the first and the second sugar residue. Core R4 has the same structure but is substituted with two Gal.[20]

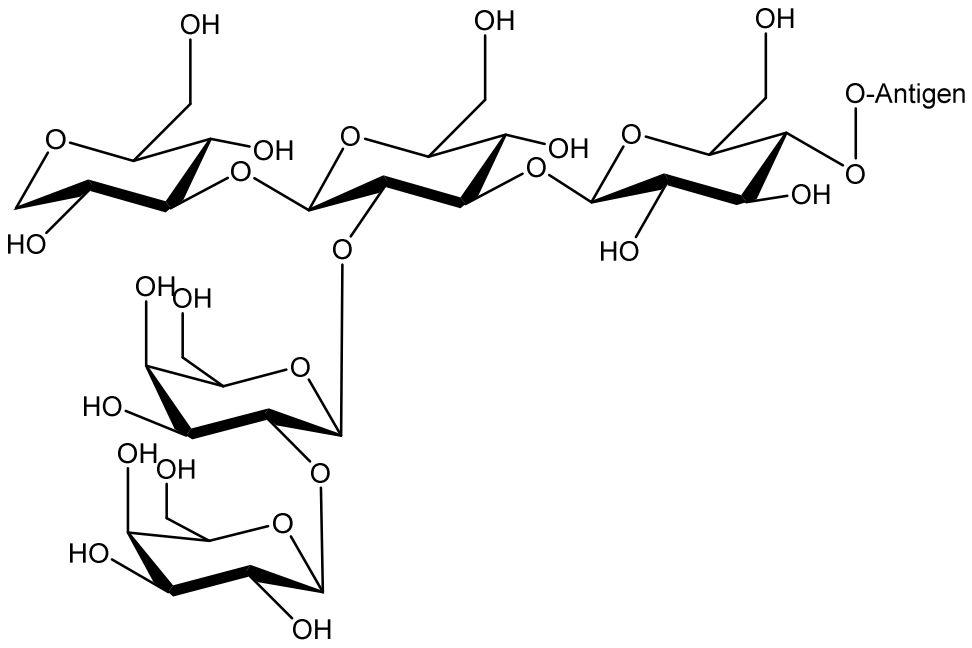

Figure 14 Structure of the hexose region of *E.coli* core R1[21][22]

The o-polysaccharide, also called o-antigen because it is specific for one serotype, is a polymer consisting of up to 50 subunits. One sugar unit is made out of 2-8 glycosyl residues. Not all LPS have the same o-polysaccharide length since during biosynthesis different lengths of subunits are polymerized and added to the LPS core. The o-antigen is exposed to cells environment, and supposed to protect the bacterium from various antibiotics and serum.[19][13]

Around 1900 Pfeiffer and Koch observed that heat-killed *Vibriocholerae* still caused toxic shocks. To differentiate between the already known exotoxins of *Vibriocholerae*, this new compound was named endotoxins. After many years and research, it was clear that those endotoxins were actually lipopolysaccharides. Endotoxins are released after lysis of gram-negative cells. They cause fever, diarrhea and sickness.[19]

3.1.2 Escherichia coli Nissle 1917

Escherichia coli Nissle 1917 (*EcN*) was isolated by Alfred Nissle in during first world war from a soldier, who was the only one of his group not having diarrhoea. A. Nissle suspected that in the soldiers gut was a strong bacteria strain present, which prevented him from enteropathogens found in this area. From the early ages on *EcN* was used for treatment of diarrhoea and similar diseases. Now *EcN* is sold as pharmaceutical preparation Mutaflor to treat inflammatory bowel diseases like Morbus Crohn or Colitis Ulcerosa.[23]

Probiotics were defined in 2011 by the World Health Organisation as “live microorganisms, which, when administered in adequate amounts, confer a health benefit on the host”.

Escherichia coli strain Nissle 1917 is a non-pathogenic *E.coli* bacterium and belongs to the *E.coli* O6-group. Its serotype is O6:K5:H1. The O6- group contains both pathogenic and non-pathogenic strains of *E.coli*, but *EcN* takes a special place. *EcN* does not produce any toxins even after administration of high dosages of *EcN*, no toxic effects could be determined.[23]

The lipopolysaccharide of *EcN* is present in a semi-rough form, which means Lipid A, the core oligosaccharide and one repeating unit of o-antigen is present. The lipopolysaccharide and the genes encoding for LPS synthesis of *EcN* were studied extensively. Several genes encoding transferases, isomerases and other enzymes for carbohydrate biosynthesis are needed for encoding LPS. In fact the o-antigen is a polymer of repeating units, which are typical for one strain. The o antigen is polymerized by the o-antigen polymerase Wzy and the o-antigen ligase links it to the core oligosaccharide. The core is added to the Lipid A in a separate manner. The presence of only one o-antigen repeating unit can be traced back to a point mutation in the gene encoding for the o-antigen polymerase Wzy.[24] *EcN*’s LPS structure has been elucidated by Grozdanov et al. Mass spectrometry proved that lipid A had a mass of 1798,4 Da, which is the typical lipid A of an *E.coli* bacterium. The backbone is phosphorylated twice, in total six fatty acids (four 3-hydroxytetradecanoic acids, one tetradecanoic acid and one dodecanoic acid) are found. The core oligosaccharide is a R1 type core, which means two KDO, two heptoses, three glucoses and two galactoses are present. The o-chain is composed of N-Acetyl-D-glucosamine linked to two mannoses with one glucose and one N-Acetyl-D-galactosamine linked to the last mannose.[24]

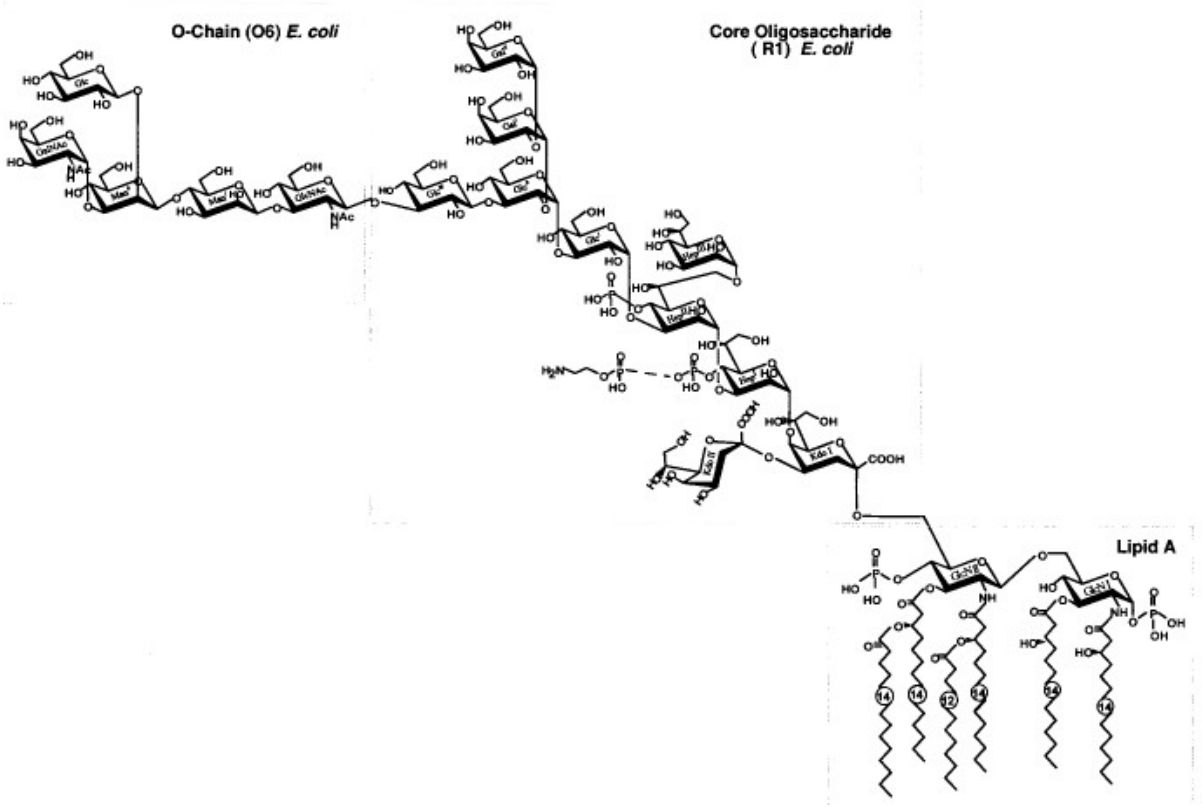

Figure 15 Lipopolysaccharide of *Escherichia coli Nissle 1917* by Grozdanov et al.[24]

EcN is does not show serum resistance, which can be explained with its short o-antigen. *EcN* does not have natural resistance against common antibiotics, expect for antibiotics, which target gram-positive cells.[23]

3.1.3 Escherichia coli BL21(DE3)

Escherichia coli BL21(DE3) is used preferably for expression of proteins. This strains has been derived from *E.coli B* and has been genetically improved so it would be usable for production of proteins.[25]

Since *BL21(DE3*) belongs to the family of *E.coli B*, their lipopolysaccharides have the same properties.[26] LPS of *BL21(DE3)* haven't been investigated, but those of *E. coli B* have already been analyzed. *E. coli B* is known to exhibit rough lipopolysaccharides with an even shorter core oligosaccharide than usual. The core is composed of only two D-glucose residues, which are present in every *E.coli* core oligosaccharide. The lipopolysaccharide of *E.coli B* is one of the shortest of *E.coli* cells. [20]

3.2 Materials and Methods

3.2.1 Chemicals and Media:

LB-Medium: Luria Broth Lennox, Roth

PBS buffer: 137 mM NaCl, 2,7 mM KCl, 12 mM Na_2HPO_4, pH= 7,5

Phenol (90%): 18 g crystalline phenol are dissolved in 2,2 mL of water

Proteinase K: 20 mg Proteinase K in 1 mL ultrapure water (100 µg/mL)

DNase:

RNase:

Other Materials:

Dialysistube: Spectra/Por Biotech Cellulose Ester MSCO 500 Da

SDS-Gels:

Table 3 SDS-PAGE Gel recipe

	Stock	**Volume**
Resolving Gel	3X Bis-Tris Buffer	5 mL
	37,5% Acrylamid	6 mL (12%)
	Water millipure	4 mL
	TEMED	25 µL
	10%APS	10 µL
Stacking Gel	1X Bis-Tris Buffer	0,75 mL
	37,5% Acrylamid	0,75 mL (4,5%)
	Water millipure	4,5 mL
	TEMED	20 µL
	10%APS	20 µL

Agar plates: 2 g LB, 1,5 g Agar in 100 mL water; additionally antibiotics if needed (50 µg/mL streptomycin, 100 µg/mL ampicillin, 50 µg/mL kanamycin)

Centricon: Amicon Ultra 0,5mL, MWCO 3 kDa

Phase lock geltube: 5 prime phase lock gel light, 1,5 mL

3.2.2 Methods

3.2.2.1 Generating streptomycin resistant *E.coli Nissle* 1917:

E.coli Nissle 1917 without resistance was grown in 25 mL-LB medium at37°C overnight. After the tube was centrifuged at 4000xg for 10 minutes, the cell pellet was resuspended in remaining LB-medium. 200 µL were streaked on two agar plates containing 50 µg/mL streptomycin. The two plates and a control plate were incubated at 37°C overnight. No colonies were detected on the control plate, but few colonies appeared on the plates containing *E.coli Nissle 1917*. Those colonies were picked and combined in 25 mL LB medium containing 50 mg/mL streptomycin, which was incubated at 37°C overnight. Again the tube was centrifuged at 4000xg for 10 minutes and the cell pellet was resuspended in the remaining LB medium. Agar-plates containing 50 µg/mL streptomycin, 100µg/mL ampicillin and 50 µg/mL kanamycin were streaked with*E.coli Nissle 1917* and incubated at 37°C overnight. Colonies occurred only on the streptomycin-plate and no other, which means that these *E.coli Nissle 1917* cells are streptomycin resistant now. The colonies were picked, an ONC containing 50 µg/mL streptomycin was incubated at 37°C and of this ONC glycerol stocks (50% glycerol, 50% cell culture) were made and stored at -80°C.

3.2.2.2 Lipopolysaccharide extraction (Hot phenol method)[27]

An overnight culture of streptomycin resistant *E.coli Nissle 1917* was incubated at 37°C in LB-medium. The cells were transferred in 1L LB medium and grown until they reached an OD_{600} of 1, which was detected by a UV-meter. The cell culture was centrifuged at 5000 rpm for 15minutes at 4°C. The cell pellet was washed using water and centrifuged at the same conditions. The cell pellet had a mass of 3,4 g and was resuspended in 20 mL of water. To gain a homogeneous suspension was transferred into a 100 mL round flask, which was placed in an oil bath heated to 68°C. The temperature of the oil bath was controlled using a thermometer. The cell suspension was stirred and equilibrated for 10 minutes, as was the 90% phenol solution. Hot Phenol was added dropwise to the suspension, which was vigorously stirred. The solution turned milky after addition of phenol. The extraction mixture was stirred at 68°C for 30 minutes. To cool down the solution quickly, the round flask was placed in an ice bath and kept there for at least 10 minutes. After centrifugation at 3500 rpm for 45 minutes at 4°C three layers were formed. The upper layer is the aqueous phase containing LPS, the layer in the middle contains parts of the cell wall and the bottom layer is the organic layer containing phenol. The aqueous phase, which had a volume of 12 mL, was removed carefully and transferred into a dialysis tubing with a cutoff of 1,0-1,2kDa. The aqueous phase was dialyzed against pure water for 3 days. The dialyzed solution was then frozen with liquid nitrogen, lyophilized and stored in -20°C.

3.2.2.3 Lipopolysaccharide extraction

Another LPS extraction was made with personal advice of Prof. Stefan Schild. Two ONCs of *E.coli Nissle 1917* with streptomycin resistance were grown for 14hours. The cells were spun down for 10 minutes at 5000 xg. The cell pellets were washed with 25 mL TMD buffer and centrifuged again. Each of them was resuspended in 1 mL TMD buffer. A vial, which is suitable for the powerlyzer, was filled with glass beads (0,25-0,5 µm) and 1 mL suspension. Cells were lyzed using the powerlyzer three times at S=34000 rpm for 1 minute. In order to get rid of the glass beads the vial was centrifuged for 5 minutes at 5000 g, the supernatant was transferred in a new tube and centrifuged for 30 seconds at 10.000 g to remove impurities. For digestion of remaining proteins, 50 µL of 20 mg/mL Proteinase K was added to the supernatant and incubated in a water bath at 55°C overnight. The solution turned from brownish-cloudy to completely clear. For phenol extraction 700 µL Phenol was added to each solution and they were transferred into a phase lock gel tube. After vortexing the mixture appears milky-cloudy. After centrifugation the upper layer, which contains LPS, was transferred in a new tube and centrifuged for 60 minutes at 75.000 xg. A white pellet is formed at the bottom, the supernatant is discarded and the pellet resuspended in TM buffer. This step is repeated once. The final pellet is resuspended in 200 µL TM buffer.

To change the buffer from TM- buffer to NMR buffer, a centricon was used. 200 µL of LPS-solution were transferred into the centricon, 200 µL of NMR buffer was added and the tube was centrifuged at 5.000 xg until 100 µL solution remained. This step was repeated 5 times, each time 400 µL NMR buffer were added.

A SDS-Gel was made before dialysis and after dialysis using all the generated fractions, so it would be clear which fraction contained LPS.

3.3 Results and Discussion

Escherichia Coli Nissle 1917 has semi-rough lipopolysaccharides on its outer cell wall.
We were able to extract those lipopolysaccharides and HSQC measurements were made to confirm the product. In an HSQC spectrum we were able to find the same peaks as Grozdanov L. et al. but we were lacking signals originating from fatty acids. It is possible that fatty acids were lost during extraction, for example due to overheating while extraction.

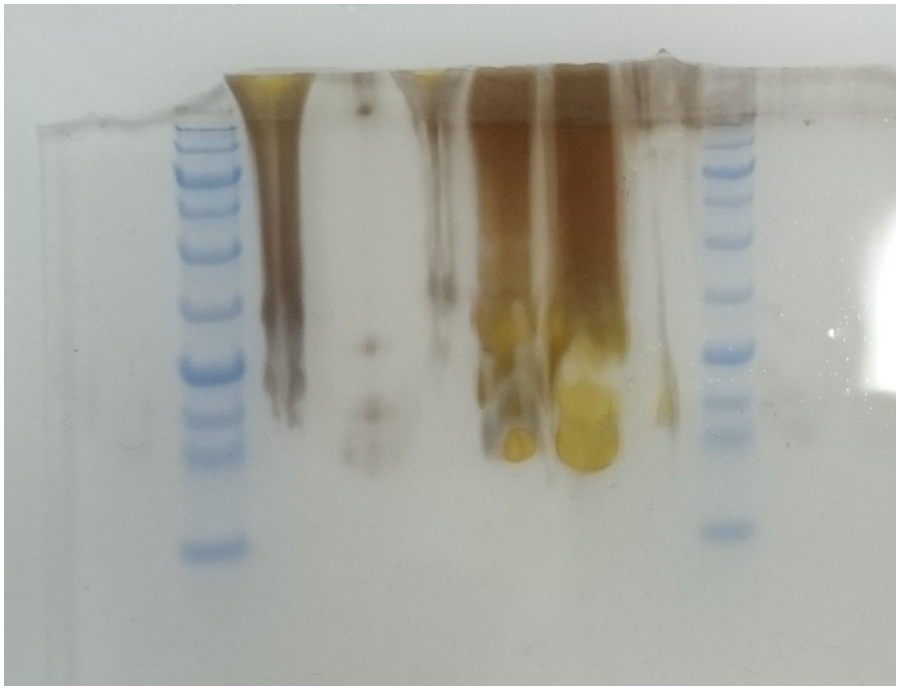

Figure 16 SDS-PAGE of *EcN* lipopolysaccharide after dialyzation, detection with silverstaining; it can be seen that many impurities are still present

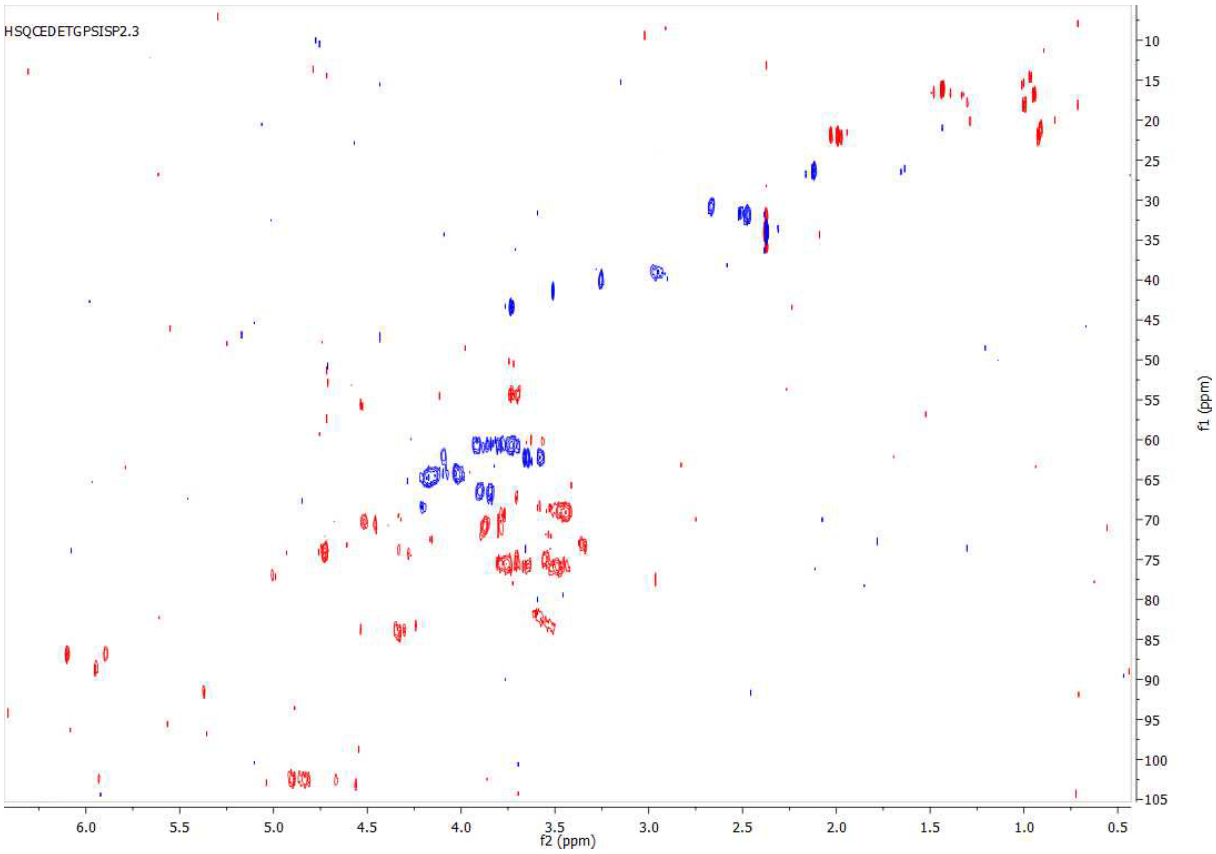

Figure 17 HSQC of lipopolysaccharides extracted from *E. coli Nissle 1917* using the hot phenol water method, after dialyzation

E.coli BL21(DE3) were grown on minimal medium, 500ul bacterial suspension (10% D2O) were used to record an HSQC. Another spectrum of isolated LPS from *E.coli BL21(DE3)* was used to compare signals. In the sugarregion (3,0-4,5 ppm) many signals are identical, hence the outer-part of LPS is detectable both as isolated product and directly on the cell as well. The spectrum of *BL21(DE3)* cells lacks lipid signals, which is presumably because lipid A is firmly fixed in the cell membrane.

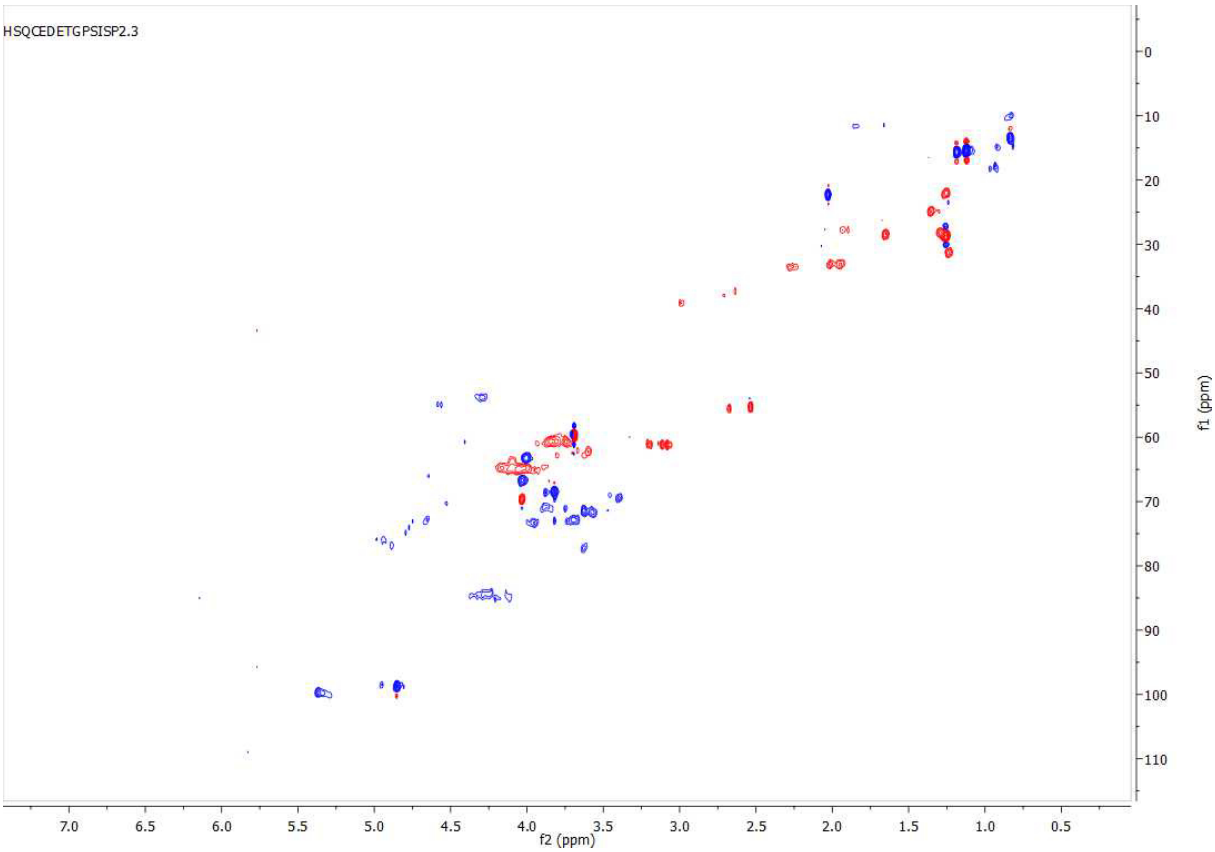

Figure 18 HSQC of living *E coli BL21(DE3)* cells

3.4 Conclusion

A method has been established for the extraction of even small lipopolysaccharides from *E. coli* cells. Gel chromatography and NMR spectra show that LPS is present, but impurities are still in the sample. Further steps will be to digest the extracted LPS with DNaseI, RNase and proteinaseK. Purification using hydrophobicity interaction or hydrophilic interaction should give very pure lipopolysaccharides.

Spectra of very pure LPS and of whole-cells can be compared and it can be proven that the structure of an o-antigen can be assigned directly from those living cells. Another possibility is to use salmonella strains, like *Salmonella enterica subsp. enterica (ex Kauffmann and Edwards 1952)* Le Minor and Popoff 1987, which exhibits LPS with many o-antigen repeating units.

Literature

[1] K. Zangger, H. Sterk, *J. Magn. Reson.* **1997**, *124*, 486–489.
[2] J. Keeler, *Understanding NMR Spectroscopy*, Wiley, Chichester, **2010**.
[3] J. Huth, R. Fu, G. Bodenhausen, *J. Magn. Reson. A* **1996**, *123*, 87–94.
[4] L. Castañar, T. Parella, *Magn. Reson. Chem.* **2015**, *53*, 399–426.
[5] K. Zangger, *Prog. Nucl. Magn. Reson. Spectrosc.* **2015**, *86-87*, 1–20.
[6] P. Sakhaii, B. Haase, W. Bermel, R. Kerssebaum, G. E. Wagner, K. Zangger, *J. Magn. Reson.* **2013**, *233*, 92–95.
[7] N. Helge Meyer, K. Zangger, *Chem Commun* **2014**, *50*, 1488–1490.
[8] J. Mauhart, S. Glanzer, P. Sakhaii, W. Bermel, K. Zangger, *J. Magn. Reson.* **2015**, *259*, 207–215.
[9] S. Glanzer, K. Zangger, *J. Am. Chem. Soc.* **2015**, *137*, 5163–5169.
[10] M. Bak, J. T. Rasmussen, N. C. Nielsen, *J. Magn. Reson.* **2000**, *147*, 296–330.
[11] T. Vosegaard, A. Malmendal, N. C. Nielsen, *Monatshefte Fr Chem. Chem. Mon.* **2002**, *133*, 1555–1574.
[12] Z. Tošner, T. Vosegaard, C. Kehlet, N. Khaneja, S. J. Glaser, N. C. Nielsen, *J. Magn. Reson.* **2009**, *197*, 120–134.
[13] C. R. H. Raetz, C. Whitfield, *Annu. Rev. Biochem.* **2002**, *71*, 635–700.
[14] L. Brown, J. M. Wolf, R. Prados-Rosales, A. Casadevall, *Nat. Rev. Microbiol.* **2015**, *13*, 620–630.
[15] M. T. Madigan, J. M. Martinko, D. A. Stahl, D. P. Clark, *Brock Mikrobiologie*, Pearson, München, **2013**.
[16] S. Qiao, Q. Luo, Y. Zhao, X. C. Zhang, Y. Huang, *Nature* **2014**, *511*, 108–111.
[17] F. Putker, M. P. Bos, J. Tommassen, *FEMS Microbiol. Rev.* **2015**, *39*, 985–1002.
[18] C. Erridge, E. Bennett-Guerrero, I. R. Poxton, *Microbes Infect.* **2002**, *4*, 837–851.
[19] M. Caroff, D. Karibian, *Carbohydr. Res.* **2003**, *338*, 2431–2447.
[20] P.-E. Jansson, B. Lindberg, A. A. Lindberg, R. Wollin, *Eur. J. Biochem.* **2005**, *115*, 571–577.
[21] D. E. Heinrichs, J. A. Yethon, C. Whitfield, *Mol. Microbiol.* **1998**, *30*, 221–232.
[22] K. Amor, D. E. Heinrichs, E. Frirdich, K. Ziebell, R. P. Johnson, C. Whitfield, *Infect. Immun.* **2000**, *68*, 1116–1124.
[23] U. Sonnenborn, J. Schulze, *Microb. Ecol. Health Dis.* **2009**, *21*, 122–158.
[24] L. Grozdanov, U. Zahringer, G. Blum-Oehler, L. Brade, A. Henne, Y. A. Knirel, U. Schombel, J. Schulze, U. Sonnenborn, G. Gottschalk, et al., *J. Bacteriol.* **2002**, *184*, 5912–5925.
[25] F. W. Studier, B. A. Moffatt, *J. Mol. Biol.* **1986**, *189*, 113–130.
[26] P. Daegelen, F. W. Studier, R. E. Lenski, S. Cure, J. F. Kim, *J. Mol. Biol.* **2009**, *394*, 634–643.
[27] "Extraction of Semi-Rough or Smooth LPS (Hot Phenol-Water Extraction)," can be found under http://glycotech.ucsd.edu/protocols/13_LPS%20Extraction_Rev2.pdf, **n.d.**
[28] K.-Y. Ahn, J.-S. Park, K.-Y. Han, J.-A. Song, J. Lee, *FEBS Lett.* **2012**, *586*, 1044–1048.
[29] J. C. Leer, K. Hammer-Jespersen, M. Schwartz, *Eur. J. Biochem.* **1977**, *75*, 217–224.
[30] A. A. Lashkov, N. E. Zhukhlistova, T. A. Seregina, A. G. Gabdulkhakov, A. M. Mikhailov, *Crystallogr. Rep.* **2011**, *56*, 560–589.
[31] F. T. Burling, R. Kniewel, J. A. Buglino, T. Chadha, A. Beckwith, C. D. Lima, *Acta Crystallogr. D Biol. Crystallogr.* **2003**, *59*, 73–76.
[32] "UniProtKB - P46857 (YRHB_ECOLI)," can be found under http://www.uniprot.org/uniprot/P46857, **n.d.**
[33] Novagen, "pcdf-1b vesctor map," can be found under http://www.helmholtz-muenchen.de/fileadmin/PEPF/pCDF_vectors/pCDF-1b_map.pdf, **n.d.**

Figure Index

Table index

Equation index

Appendix

During my research on pure shift NMR and its applications, I worked on a side project dealing with protein-protein interactions. Interaction studies of biological macromolecules using NMR are a possible field for application of pure-shift NMR. It was proposed that the small protein YrhB protects the activity of uridine phosphorylase after heat shock.[28] These two proteins are purified and activity assays as well as interaction studies are performed to verify the published results.

1 Uridine phosphorylase and YrhB

1.1 Introduction

Uridine phosphorylase (UDP), a biologically very important enzyme, and YRHB, an uncharacterized protein, were purified. The activity of UDP in absence and presence of YRHB towards uridine was determined by NMR and with classical activity assays.

1.1.1 Uridine phosphorylase

The enzymes uridine phosphorylase (UDP), thymidine phosphorylase and purine nucleoside phosphorylaseare essential for nucleotide synthesis.[29]UDP is shown to be present in prokaryotes, as well as yeast and higher organisms.[30].
UDP catalyzes the reaction of uridine and phosphate to uracil and alpha-D-ribose-1-phosphate. Here the C-N glycosidic bond cleaved and the ribose-moiety is phosphorylated.

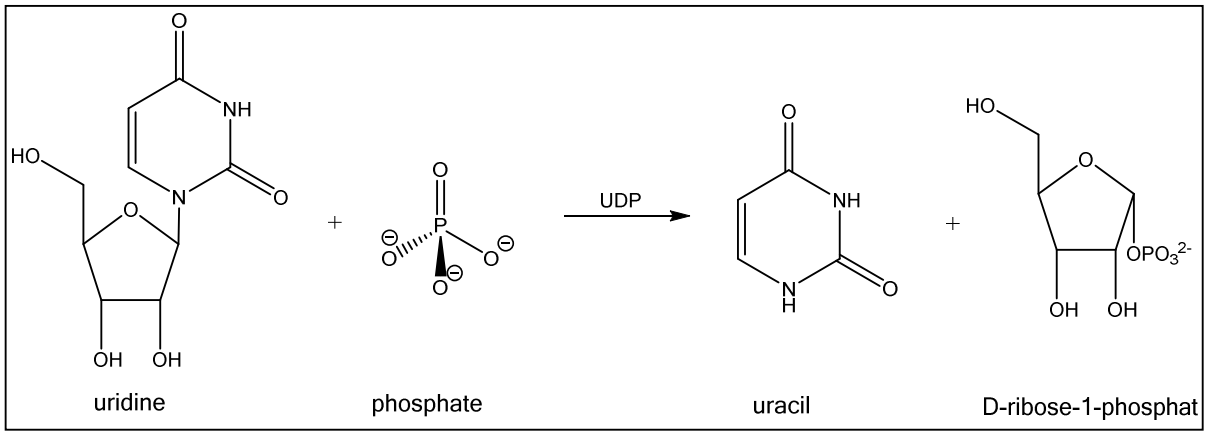

Figure 19 Uridine phosphorylase catalyzes the degradation of uridine to uracil and D-ribose-1-phosphate

This reaction is important in the pyrimidine metabolism pathway. In *Escherichia coli* the product ribose-1-phosphate is further phosphorylated to ribose-5-phosphate, which is used in

the pentose metabolism. The second product uracil is converted into UMP (uracil monophosphate), which is a precurser for RNA synthesis.[29]

In *Escherichia coli* uridine phosphorylase exists as a hexamer with a molecular weight of ZITAT, each monomer consisting of 253 amino acids.[30] It was shown that the active site of one monomer receives three residues from the neighbouring monomer. This is an indication that a dimer is needed in order to form a functional active site.[31]

1.1.2 YrhB

YrhB is an uncharacterized protein found in *Escherichia coli K12*.[32] Its molecular mass is 10,6 kDa, which makes it a small protein. According to K.-Y.Ahn et al.[28]it is believed that YrhB has chaperone-like activities and has heat-resistant features. They claim that presence of YrhB in cells increased after giving them a heat-shock (48°C). Therefore they suspect this protein has a cellular function connected to heat shock stress. They investigated YrhB's role of preventing aggregation of PurK caused by heat and its role in the refolding of UP. Their activity analysis of UP revealed that YRHB has a positive effect on refolded UDP's activity towards uridine.[28]

1.2 Materials and Methods

1.2.1 Materials for YRHB purification

1.2.1.1 1 L M9 minimal-medium (^{15}N labelled):

0,7 g ($^{15}NH_4$)Cl
3,0 g Glucose
1 mL $MgSO_4$ 1M1 mL Microsalts-stock (150 mM $CaCl_2$, 20 mM $FeCl_3$, 50 mM H_3BO_3, 150 µM $CoCl_2$, 800 µM $CuCl_2$, 1 mM $MnCl_2$, 1,5 mM $ZnCl_2$, 15 µM $(NH_4)_6Mo_7O_{24}$*$4H_2O$)
1 mL Vitamin-stock (1 mg/mL Biotin, 1 mg/mL Thiamin)
1 mL Antibiotics-stock (Ampicillin: 100 mg/mL; Streptomycin: 75 mg/mL)

1.2.1.2 Columns:

Table 4 FPLC columns used for purification of YRHB

Column	Type	Properties
Hitrap Q HP	Ion exchange	Hitrap Q-HP, GE Healthcare; 2x 5 mL;
Hitrap Phenyl FF	Hydrophobic interaction	Phenyl FF, GE Healthcare; 2x 5 mL; Phenyl on Sepharose
SEC Superdex 75	Size exclusion	HiLoad 26x600 mm, Superdex 75 pg, 320 mL

1.2.1.3 Buffers:

Table 5 Buffers used for FPLC purification of YRHB and dialysis buffer

Hitrap Q HP	Buffer A: 50 mM Na_2HPO_4 50 mM NaCl, 0,02% NaN_3 pH= 8,0
	Buffer B: 50 mM Na_2HPO_4 1 M NaCl, 0,02% NaN_3 pH= 8,0
HitrapPhenyl FF	Buffer C: 50 mM Na_2HPO_4, 1,5 M $(NH_4)_2SO_4$
	Buffer D: 50 mM Na_2HPO_4, 0,02% NaN_3 pH= 8,0
SEC (Superdex 75, Superdex 200)	Buffer E: 50 mM Na_2HPO_4, 300 mM NaCl
	Buffer F: : 50 mM Na_2HPO_4, pH= 8,0
Dialyzing-Buffer	50mM Na_2HPO_4 100 mM NaCl pH= 6,5

1.2.1.4 FPLC column run programs:

Hitrap Q equilibration:

Isocratic flow	100% Buffer A	50 mL	4 mL/min
Isocratic flow	100% Buffer B	50 mL	4 mL/min
Isocratic flow	100% Buffer A	50 mL	4 mL/min

Hitrap Q run:

Isocratic flow	100% Buffer A	12 mL	3 mL/min
Zero Baseline			
Linear Gradient	100% Buffer A → 0% Buffer A 0% Buffer B → 100% Buffer B	200 mL	3 ml/min
Isocratic flow	100% Buffer B	50 mL	3 mL/min

Fractions of 4 mL were collected during the entire run.

Hitrap Phenyl FF equilibration:

Isocratic flow	100% Buffer D	50 mL	3 mL/min
Isocratic flow	100% Buffer C	50 mL	3 mL/min

Hitrap Phenyl FF run:

Isocratic flow	100% Buffer C	50 mL	3 mL/min
Zero Baseline			
Linear Gradient	100% Buffer C →0% Buffer C 0% Buffer D → 100% Buffer D	200 mL	3 mL/min
Isocratic flow	100% Buffer D	60 mL	3 mL/min

Fractions of 3,00 mL were collected during the entire run.

SEC Sephadex 75 equilibration and run:

Isocratic flow	100% Buffer E	400 mL	2 mL/min
Zero baseline			
Load/Inject Sample	100% Buffer E	50 mL	2 ml/min
Isocratic Flow	100%Buffer E	350 mL	2 mL/min
Isocratic Flow	100% Buffer F	1000 mL	2 mL/min

The static loop had a volume of 10 mL, fractions of 4 mL were collected during minute 225 and 390.

1.2.1.5 SDS-PAGE Gel:

Table 6 SDS-Page gel recipe for 12% acrylamide gels

	Stock	**Final concentration**
Resolving Gel	3X Bis-Tris Buffer	5 mL
	37,5% Acrylamid	4,68 mL (12%)
	Water Millipore	5,32 mL
	TEMED	10 µL
	10%APS	25 µL
Stacking Gel	1X Bis-Tris Buffer	0,75 mL
	37,5% Acrylamid	0,75 mL (4,5%)
	Water Millipore	4,5 mL
	TEMED	20 µL
	10%APS	20 µL

1.2.1.6 Buffers for SDS-PAGE:

1X MES Running Buffer: 50 mM 2-(N-morpholino)ethanesulfonic acid

Comassie Blue staining solution

Destaining solution: 45% Ethanol, 45% H_2O, 10% acetic acid

1.2.2 Method for purification of YRHB

E. Coli BL21(DE3) were grown at 37°C in minimal media. When the optical density at 660nm reached 0,56, protein expression was induced with 1mL of 1mM IPTG. After 4 hours of cultivation, the cells were harvested by centrifugation, washed with 5mL PBS-Buffer and centrifuged again. Cells were frozen with liquid nitrogen and stored at -20°C.

After resuspending the cell pellet in 25ml buffer, protease inhibitor was added and the cells were lysed using a French press (2000, twice) and centrifuged for 1h at 9900 rpm. The

supernatant was filtered and loaded onto an equilibrated Hitrap Q-HP column. The protein was eluted with a gradient from bufferA to buffer B.

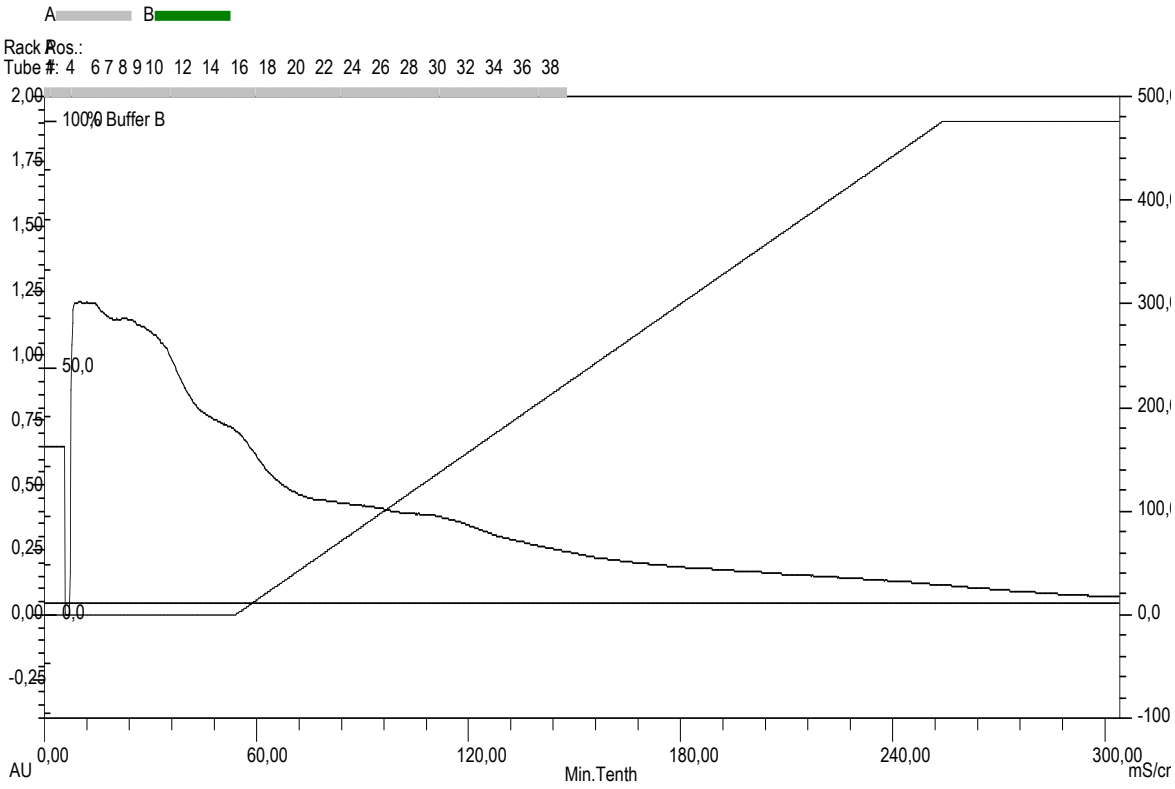

Figure20 Chromatographic profile of YrhB on a HiTrap Q column

For Saltprecipitation fractions were pooled and Ammoniumsulfate was added to a concentration of 1,5mol/L and the solution was centrifuged for 1 hour at 20000xg. The supernatant was filtered and loaded onto an equilibrated Phenyl FF column and eluted with buffer D.

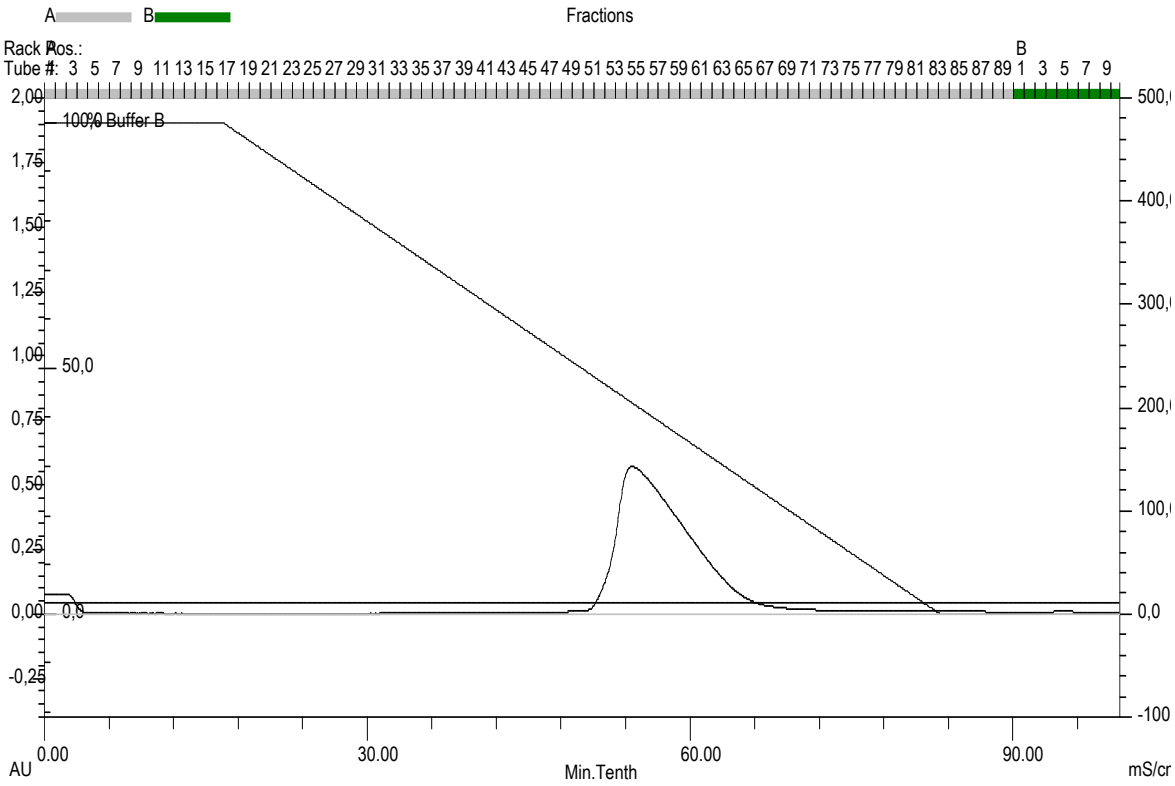

Figure21ChromatographicprofileofYrhB on a HiTrap Phenyl FF column

Fractions were pooled, filtered and concentrated using anAmicon® Ultra 4mL Filterand then loaded onto an equilibrated size exclusion column (sephadex 75). Protein was eluted with buffer F.

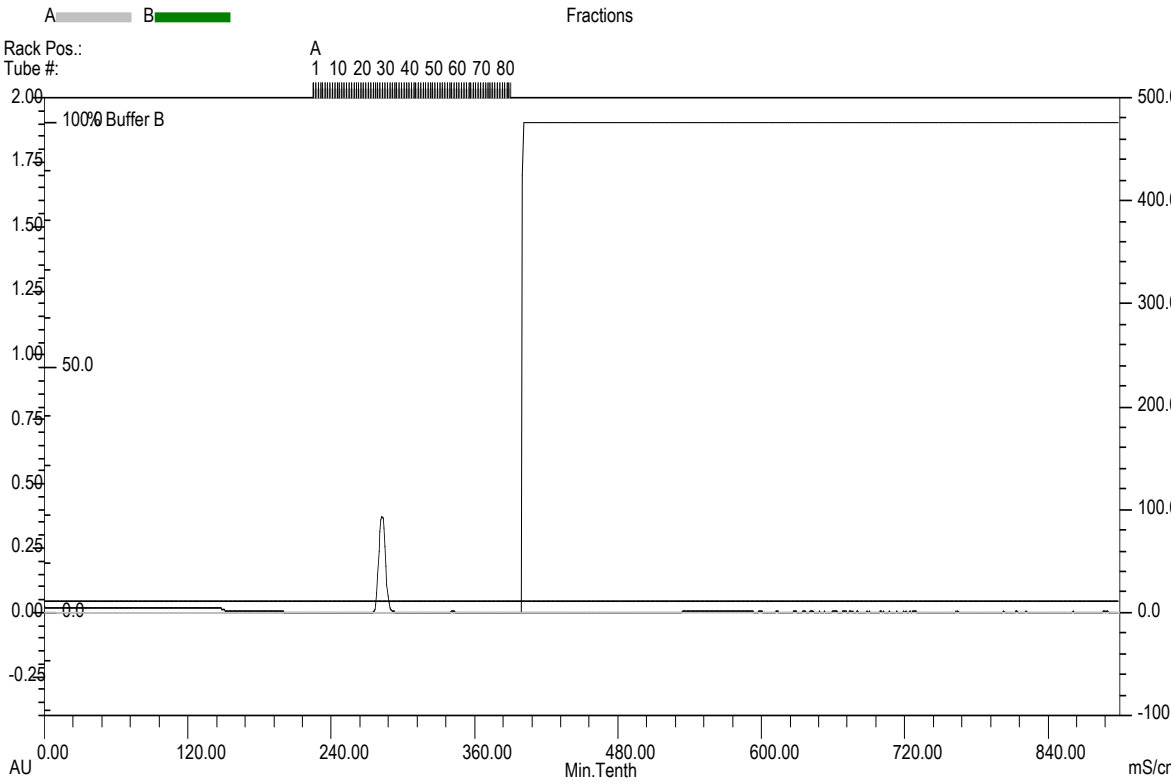

Figure22ChromatographicprofileofYrhB on a SEC Superdex 75

Fractions were pooled and dialyzed against dialyzing-buffer for 4 days with changing the buffer at the second day. The dialyzed sample was concentrated by anAmicon® Ultra 4mL Filter, frozen with nitrogen and stored at 20°C. The YRHB was defrosted once UDP was purified and dialyzed against dialyzing-buffer to achieve identical buffer conditions. Further YRHB was concentrated to 4,230 mg/mL (392 mM).

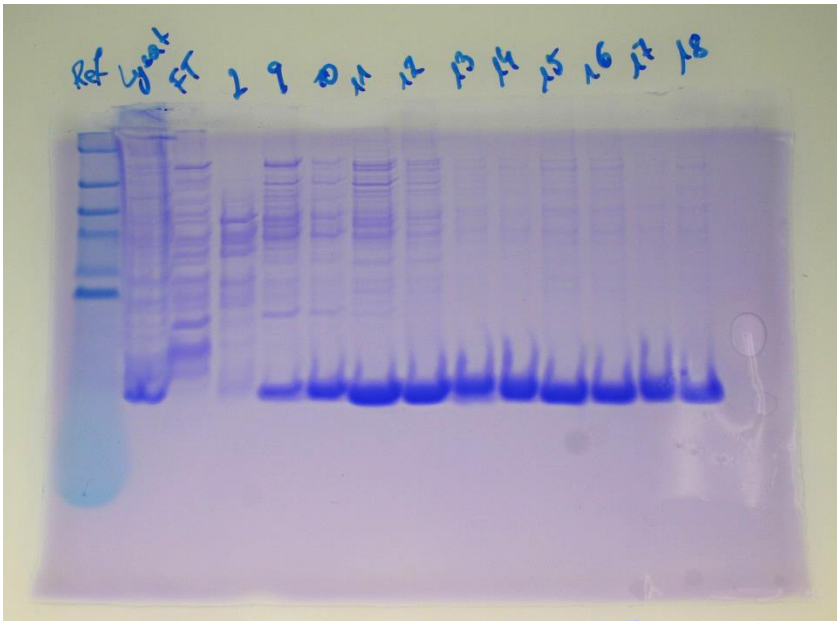

Figure 23 SDS-Page of YrhB after HiTrap Q column, cell lysate and flow through of loading the column

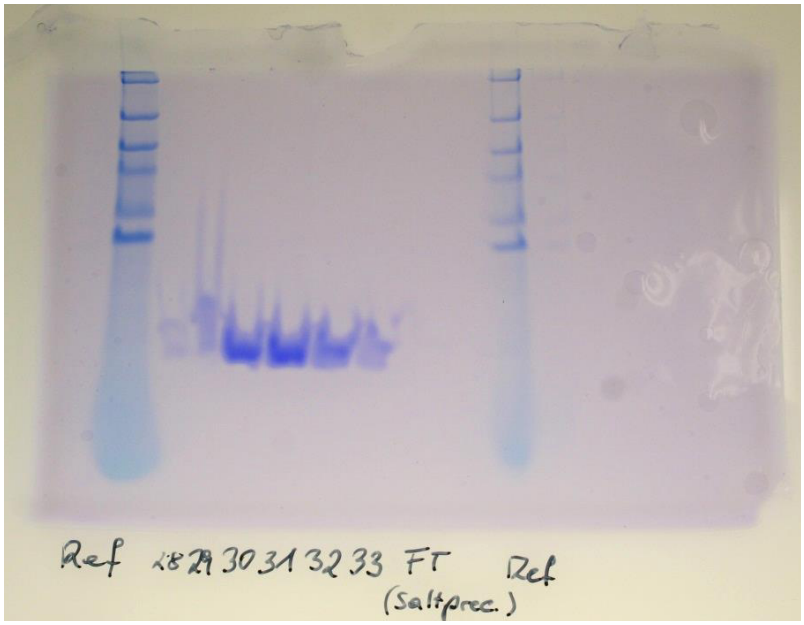

Figure 24 SDS-Page of YrhB after SEC chromatography and Flow through after salt precipitation

1.2.3 Materials for UDP

1.2.3.1 Plasmids and vectors:

Plasmid pcdf-1b[33]

For Extraction: QuiagenMiniprep Plasmid Kit 2

Vector:

MSKSDVFHLG LTKNDLQGAT LAIVPGDPDR VEKIAALMDK PVKLASHREF
TTWRAELDGK PVIVCSTGIG GPSTSIAVEE LAQLGIRTFL RIGTTGAIQP
HINVGDVLVT TASVRLDGAS LHFAPLEFPA VADFECTTAL VEAAKSIGAT
THVGVTASSD TFYPGQERYD TYSGRVVRHF KGSMEEWQAM GVMNYEMESA
TLLTMCASQG LRAGMVAGVI VNRTQQEIPN AETMKQTESH AVKIVVEAAR
RLL

1.2.3.2 Primer and cutting enzymes:

Forward primer (5‘-3‘):

CCA TCA CGT GGG TAC CAT GTC CAA GTC TGA TGT TTT TCA TCT C

Reverse primer (5’-3’):

TCG AGT GCG GCC GCA AGC TTT TAC AGC AGA CGA CGC GC

Cutting enzymes:

Kpn1

Hind3

1.2.3.3 Bacterial strains:

BL21(DE3)

DH5α

1.2.3.4 DNA-Gel:

Agarose 1%
TAE 1%
Loading Dye: peqGREEN non-toxic DNS/RNA dye

DNA Ladder: 2-log DNS ladder (0,1-10 kb)

1.2.3.5 Chromatography columns

Table 7 Chromatographic columns for purification of UDP

Column	Type	Properties
Ni-NTA resin	Affinity chromatography	Ni-NTA agarosefromQiagen
SEC superdex 200	Size exclusion	HiLoad 16x600 mm, Superdex 200 pg, 120 mL

1.2.3.6 Buffer:

Table 8 Buffers used for chromatographic purification of UDP

Ni-NTA resin	Wash 1	20 mM Tris pH= 8,0 10 mM Imidazole 150 mM NaCl 2mM β-Mercaptoethanol
	Wash 2	20 mM Tris pH= 8,0 10 mM Imidazole 150 mM NaCl 2mM β-Mercaptoethanol
	Wash 3	20 mM Tris pH= 8,0 10 mM Imidazole 1 M NaCl 2mM β-Mercaptoethanol
	Wash 4	20 mM Tris pH= 8,0 20 mM Imidazole 150 mM NaCl 2mM β-Mercaptoethanol
	Elution	20 mM Tris pH= 8,0 330 mM Imidazole 150 mM NaCl 2mM β-Mercaptoethanol
SEC Superdex 200	Buffer A	: 50 mM Na_2HPO_4, 300 mM NaCl, pH= 8,0
	Buffer B	50 mM Na_2HPO_4, pH= 8,0

1.2.3.7 FPLC column run programs

SEC Sephadex 200 equilibration and run:

Isocratic flow	100% Buffer E	400 mL	2 mL/min
Zero baseline			
Load/Inject Sample	100% Buffer E	50 mL	2 ml/min
Isocratic Flow	100%Buffer E	350 mL	2 mL/min
Isocratic Flow	100% Buffer F	1000 mL	2 mL/min

The static loop had a volume of 10 mL, fractions of 2 mL were collected during hour 8 and hour 10.

1.2.4 Methods for UDP

1.2.4.1 PCR – Polymerase chainreaction:

6 reactions of each 50µL were made, they contained:

1X Buffer
100 µM dNTP
0,25 µM Primer forward
0,25 µM Primer reverse
1 µM Polymerase Q5
20 ng Template

One of 6 reactions was a control reaction, which contained every component except for the template. The PCR conditions were selected according to the properties of primers and the amplified DNA.

PCR Cylce:

1) 98°C, 5 minutes
    - Start of cycle
2) 98°C, 1 minute
3) 60°C, 30seconds
4) 72°C, 30 seconds
    - End of cycle
5) 72°C, 2 minutes

1.2.4.1.1 Restriction digestion:

43 µL of pcdf-1b plasmid (25 ng/mL) was mixed with 1 µL of each KpnI and HindIII in 5 µL of 10X CutSmart Buffer. This mixture was incubated at 37°C for 30 minutes, then 1 µL Phosphatase was added and it was again kept at 37°C for 30 minutes. Afterwards the mixture was loaded on a DNA agarose Gel and separated for 30 minutes at 130 V. The DNA-band was cut out and the DNA was extracted with the DNA extraction kit.

46 µL of PCR-product was cut with each 2 µL KpnI and HindIII in 5,5 µL 10X CutSmart Buffer for 30 minutes at 37°C, then 1 µL Phosphatase was added and the mixture was kept at 37°C for additional 30 minutes. The mixture was loaded on a DNA agarose gel, run for 30 minutes

at 130V. The DNA-band was cut out of the gel and extracted using the same Gel extraction kit.

1.2.4.2 Ligation and transformation:

The ligation was carried out with two different volumes of insert DNA, the final volume was always 20 µL.

Table 9 Volumes used for ligation

Plasmid [6,2 ng/ µL]	Insert DNA [13,6 ng/ µL]	LB	Ligase	H_2O
5,4 µL	1 µL	2 µL	1 µL	10,6 µL
5,4 µL	5 µL	2 µL	1 µL	6,6 µL

The mixture was incubated at 16°C.
For transforming the DNA into living cells, DH5α cells were defrosted on ice, then 10 µL of DNA was added and it was kept on ice for 30 minutes. After a heat shock (42°C) for 30 seconds, the cells were put on ice immediately and SOC-Medium was added. The cells were incubated at 37°C for 1 hour, and then they were spun down and plated on LB-plates with streptomycin. The LB-plates were kept at 37°C for 2 nights.
Only on one plate colonies were found, because the ligation using 1 µL of insert DNA did not work. From the colonies (of the ligation using 5 µL insert DNA) an ONC was made. The plasmid was extracted using the micro extraction kit 2, and it was transformed into BL21(DE3) cells using the technique described above. From colonies of BL21(DE3) containing the UDP expression vector, three ONC were cultivated and glycerol stocks were made.

1.2.4.3 Purification of UDP:

UDP was purified as previous described.[31] *E.coli BL21(DE3)* were grown in 1L LB Medium until an OD of 0,6 was reached. Then protein expression was induced by addition of 1 mL IPTG (1 mM). After additional 4 hours of cultivation, cells were centrifuged at 5000 rpm for 15 minutes. Cells were resuspended in 25 mL “Wash1”-Buffer, 100 µL protease inhibitor was added, and sonicated on ice at 40% amplitude, 2seconds on/off, for 25 minutes. The lysate was centrifuged at 9900 rpm for 1 hour, the supernatant was removed and filtered. A Ni-NTA-agarose resin was equilibrated and loaded with the lysate. After washing with 2 times 10 mL washbuffer 1, 10 ml washbuffer 2, 10 ml wash buffer 3, an 10 ml wash buffer 4, the protein was eluted with 10 ml elution buffer. The elution was loaded onto an equilibrated size exclusion column (sephadex 200) and a UDP was eluted with buffer B.

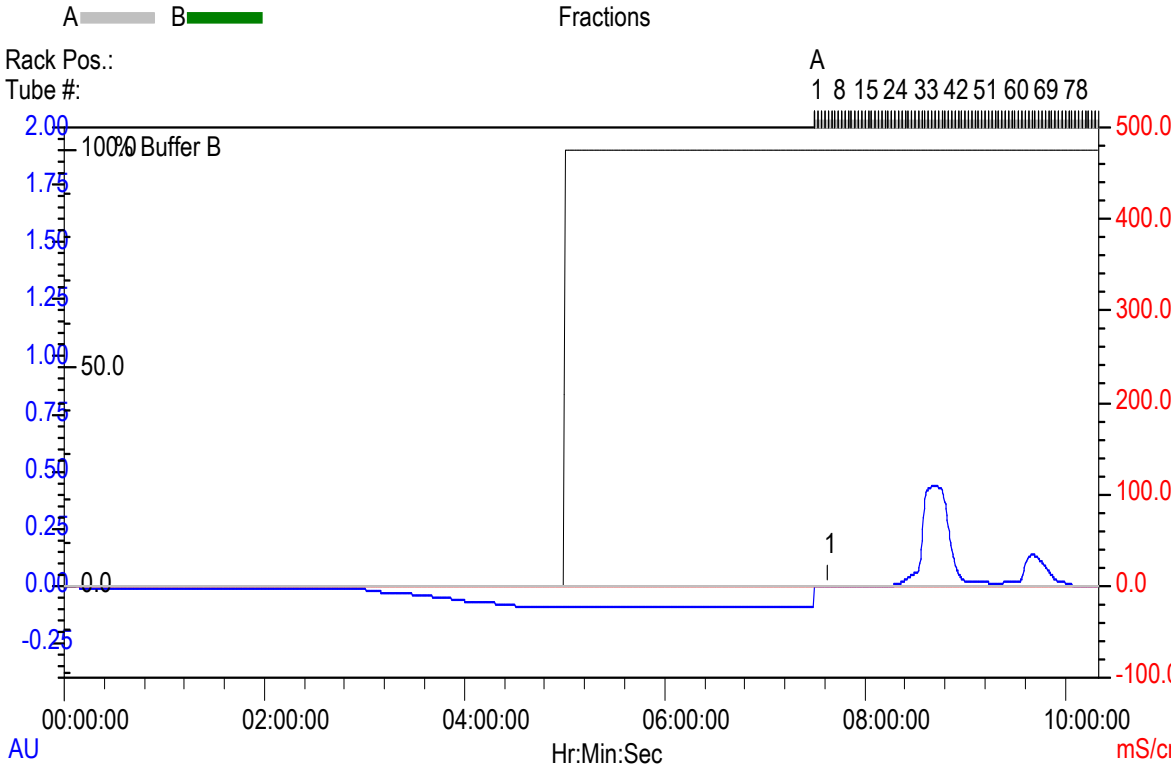

Figure25Chromatographicprofileof UDP after SEC

The fractions were analyzed by SDS-PAGE. The pooled fractions of UDP as well as the defrosted YRHB-solution were dialyzed against dialyzing buffer in order to get the exact same buffer conditions. The UDP fractions were concentrated to a concentration of 11,328 mg/mL (417 nM).

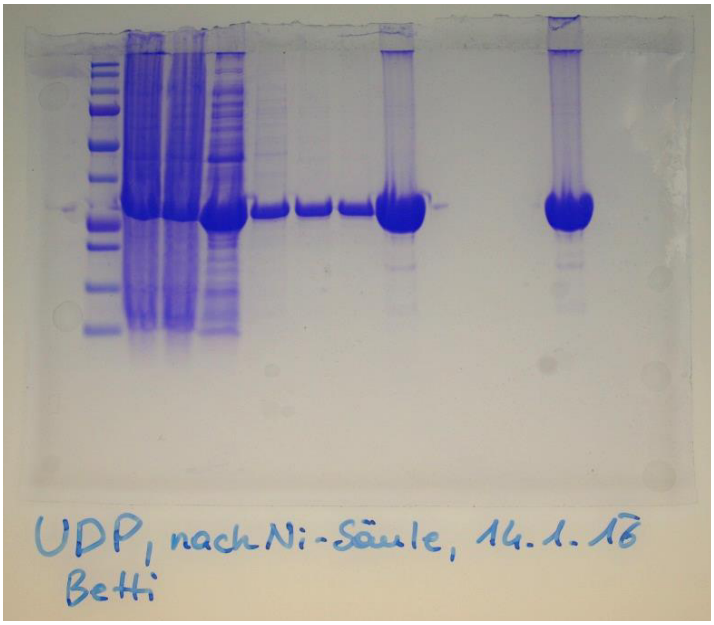

Figure 26 UDP after Ni-NTA resin, W1, W2, W3, W4, W5

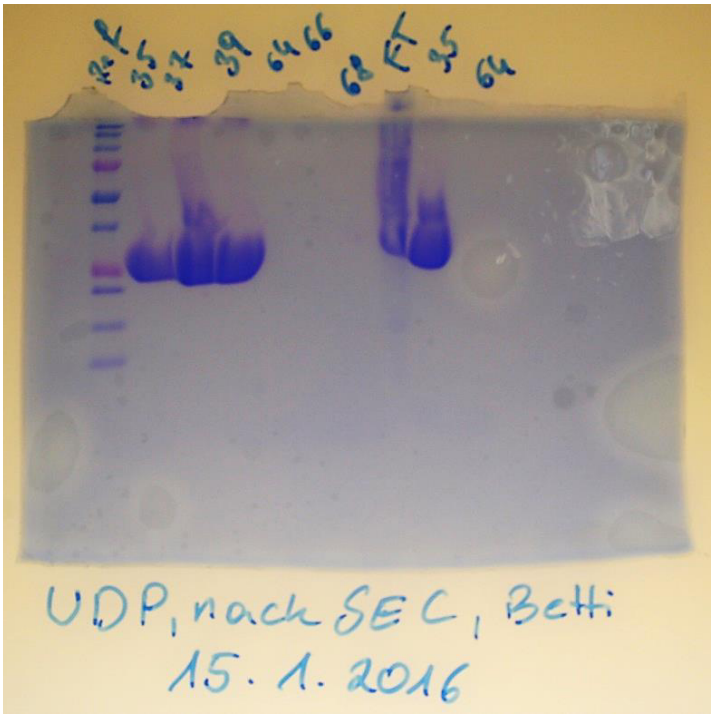

Figure 27 Fractions of UDP after SEC

1.2.4.4 Activity Assay of UDP:

The activity assay was performed for two temperatures according to the previous report of Leer et al.[29]. The reaction buffer contained 5 mM uridine, 10 mM phosphate, 10 mM Tris-HCl and 1 mM EDTA at pH 7,3.

For the assay at 25°C, 950 µL of reaction buffer were mixed with 50 µL of protein solutions of different concentrations. UDP was added in concentrations of 2 µM and 400 nM. Further a mixture of both UDP and YRHB in a concentration of 400 nM as well as YRHB in 400 nM was used as a control. The mixture of reaction buffer and protein were incubated at 25°C. Every five minutes a sample of 30 µL was taken and added to 70 µL of 0,5 M NaOH to stop the reaction.

For monitoring the reaction at 60°C, 1 mL samples containing 2 µM/ 400 nM UDP or 400 nM UDP+YRHB were placed in a heating block. Every five minutes 25 µL of the samples were added to 475 µL reaction buffer. UDP was allowed to react for 5 minutes, then 30 µL of reaction solution was added to 70 µL 0,5 M NaOH.

The absorbance of uracil was read at 290 nm.

1.3 Results

1.3.1 Activity assay

Activity assays were made for different concentrations of UDP at different temperatures. Additionally a mixture of UDP and YRHB was made. The absorption at 290 nm was measured and as a standard ΔA_{290}=5,41 for 1 mM uracil was taken. (Leer, Hammer-Jespersen, Schwartz, 1976)

For a concentration of 400 nM UDP at 25°C a reaction rate of 0,38 nMs^{-1} was calculated. As it is shown in the graph, the absorption and hence the concentration of uracil, is increasing linearly because UDP has more time for catalyzing the reaction. At 60°C we expect a decrease of absorption, because UDP gets inactivated by heat and therefore its activity in 5 minutes reaction time decreases.

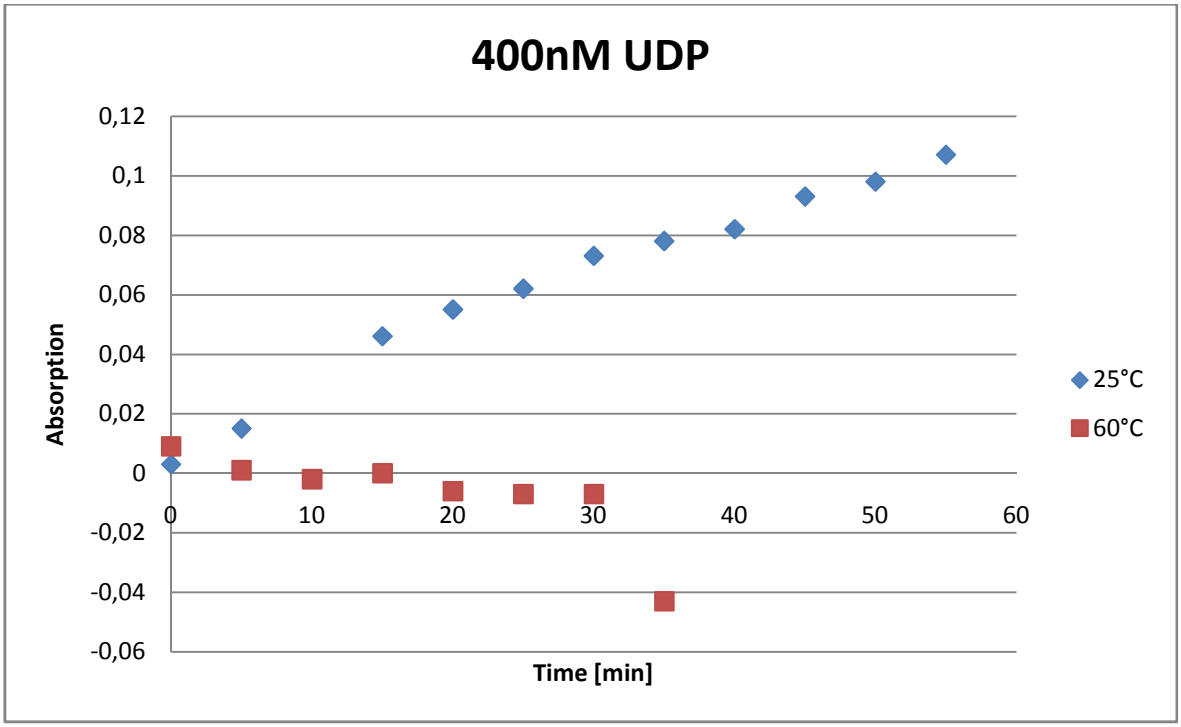

Figure 28 Activity of 400nM UDP over a time span of 40 minutes at 25°C and 60°C; absorption of uracil was measured

The activity-curve of UDP decreases very fast and after 10 minutes incubation at 60°C no activity of the protein is left. UDP is not heat stable at all.

A reaction constant of 0,60 nMs^{-1} in the 2 µM solution of UDP was calculated for 25°C. For the experiment at 60°C we see clearly a loss of activity during the first 10 minutes, afterwards the activity stays at zero. The concentrations in which UDP is used do not influence the stability over time

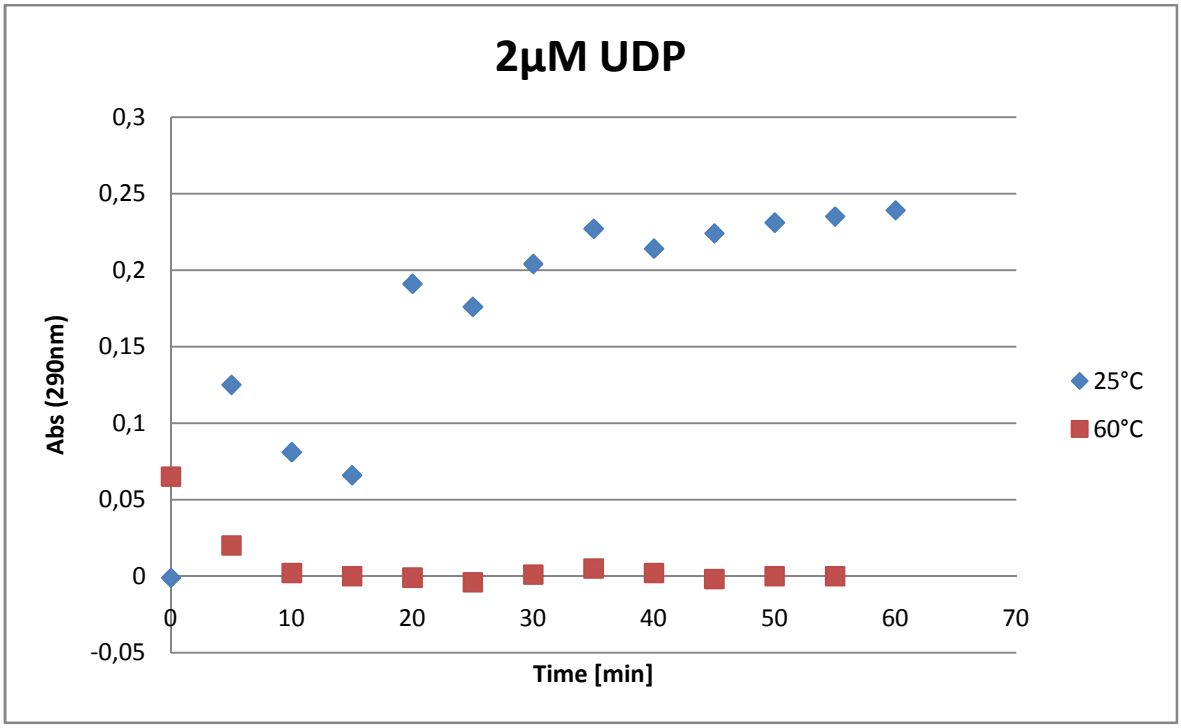

Figure 29 Activity of 2µM UDP over a time span of 60 minutes at 25°C and 60°C; absorption of uracil was measured

An experiment at 25°C where the reaction solution contained 400 nM UDP and 400 nM YRHB showed that YRHB has no activity towards uridine itself. The similar curves of UDP and UDP+YRHB indicate that YRHB does not change UDP's activity.

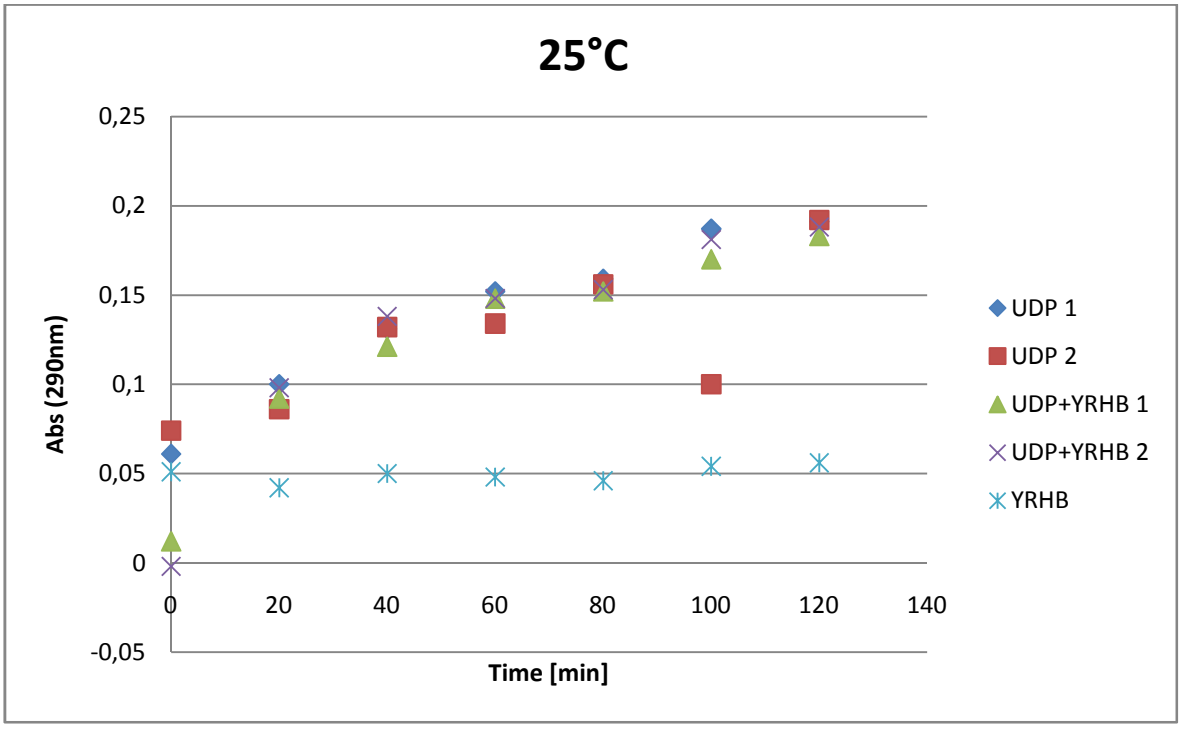

Figure 30 Absorption of uracil, product of the UDP-catalyzed reaction at 25°C; UDP as catalyst, UDP+YrhB as catalyst-mixture and YrhB as control are displayed

Looking at the experiment with YRHB and UDP at 60°C we see that all curves decrease with the same rate, so there is no influence of YRHB on UDP present. Because of using a wrong blank the curves lower limit is around 0,05 absorption units.

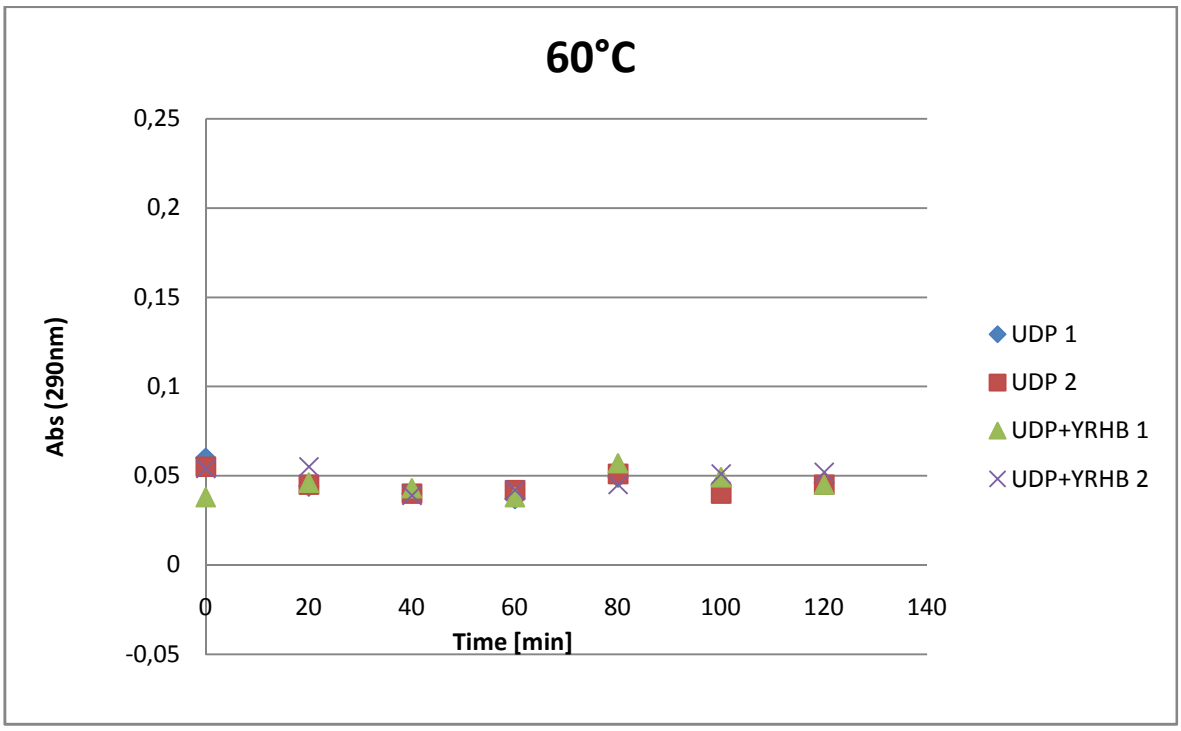

Figure 31 Absorption of uracil, product of the UDP-catalyzed reaction at 60°C; UDP as catalyst, UDP+YrhB as catalyst-mixture and YrhB as control are displayed

1.3.2 NMR Spectroscopy

An HSQC of YRHB was recorded at 300 K as a standard. Further an HSQC of a sample containing UDP and YRHB was measured at the same temperature. For investigation of a possible interaction between the two proteins at 362,2°C, the spectrometer was heated until a constant temperature was reached. Each sample was equilibrated for 10 minutes at 362,2 °C. To see changes with time HSQCs and 1D-spectra were recorded alternating for 2 hours for both samples.

Altogether 6 HSQC spectra were recorded for each sample and we could not see a difference in those spectra. Comparing the spectra of two temperatures we see some peak shifts due to the temperature change but mostly it can be seen that the signal intensity of the spectrum decreases due to decrease of protein concentration.The same effect was observed for a sample containing only YrhB. Therefore there is no visible interaction between YRHB and UDP.

For proving that both proteins were present in the measured solution, a SDS-Gel was prepared.

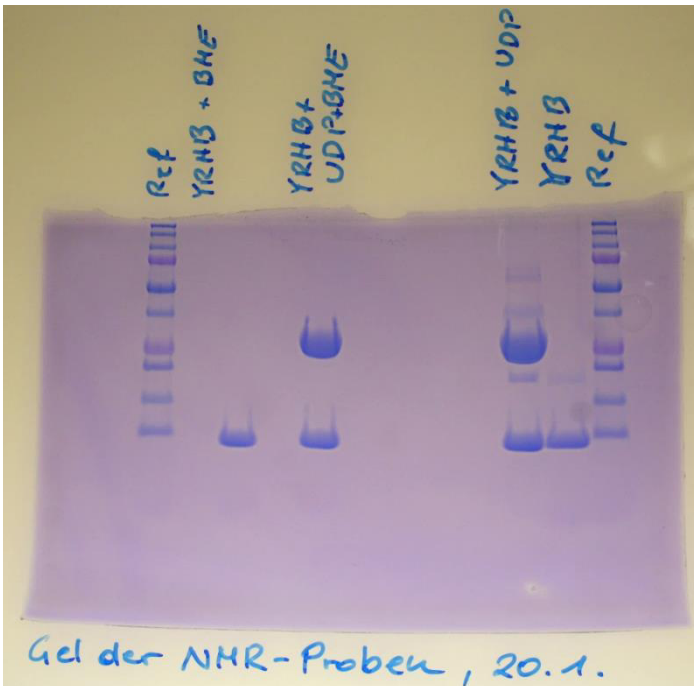

Figure 32 SDS-PAGE Gel of the samples used for NMR spectroscopy

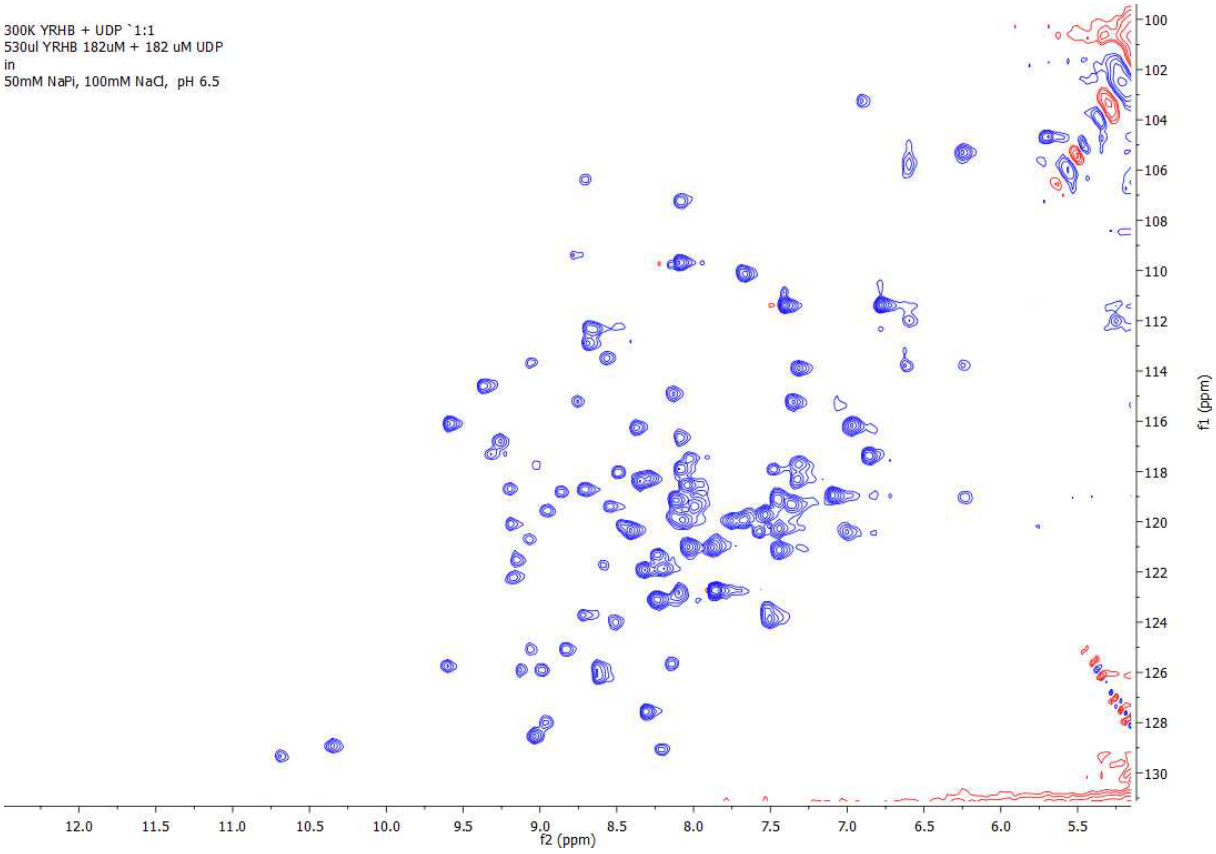

Figure 33 HSQC spectrum of a mixture of UDP and YrhB (181 µM) at 300 K

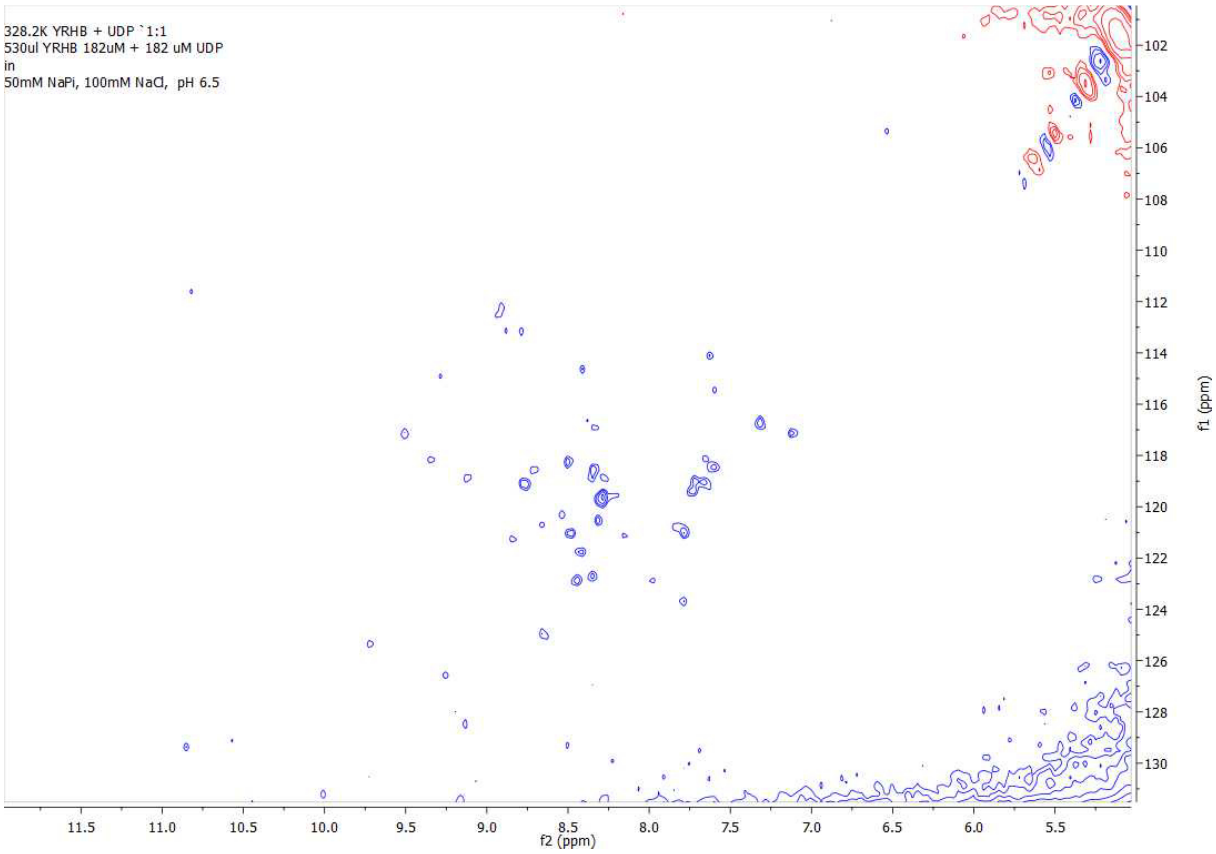

Figure 34 HSQC of UDP and YRHB after being incubated for 10 hours at 328 K.

2 Strong coupling

A spinsystem oft wo protons was simulated with SIMPSON: In the next chapters the script, which was used, is shown. The parameters defining the spinsystem are found in the section “spinsys”. The parameters shift 1, shift 2 and jcoupling have been altered to simulate different strengths of strong coupling as can be seen in the figures in 2.2.3. For each spinsystem, a density matrix has been calculated.

2.1 SIMPSON Script

```
# spectrum of 2 strongly coupled protons
spinsys {
        channels 1H
        nuclei 1H 1H
        shift 1 0 0 0 0 0 0
        shift 2 0 0 0 0 0 0
        jcoupling 1 2 50 0 0 0 0 0
}


source ./util.tcl

par {
        method          direct freq

        crystal_file    alpha0beta0
        gamma_angles    1
        spin_rate       0

        sw              1000
        np              32768
        proton_frequency 500e6
        start_operator  I1z + I2z
        detect_operator  I1p + I2p
        variablerf    150000

}
```

```
procpulseq {} {
        global par

        set t180 [expr 0.5e+6/$par(rf)]
        set t90 [expr 0.25e+6/$par(rf)]
        set t [expr 2*$par(np)/$par(sw)]
        reset

        puts "start matrix:"
        putmatrix [matrix get start]
        puts "90pulse + delay 100 + 180pulse"

        pulse $t90 $par(rf) 90
        delay 1000
        pulse $t180 $par(rf) 0
        delay 1000


        acq_block {
            delay $t
        }


        puts "after multiple pulses:"
        putmatrix [matrix get density]

}

proc main {} {
global par

set f [fsimpson]

puts "t90 = [expr 0.25e+6/$par(rf)]"
  set lb [expr 10.0*$par(sw)/$par(np)]
```

```
# line-broadening is done in time domain
fft $f -inv
faddlb $f $lb 0

fft $f
# here we use custom Fsave function defined in ./util.tcl
setspename [Fsave $f $par(name)]
puts "Saved files: $spename"
funload $f
}
```

2.2 Density matrices for different chemical shift differences

J=50 Hz; v1=0 Hz, v2=100 Hz

start matrix:

(1, 0) (0, 0) (0, 0) (0, 0)
(0, 0) (0, 0) (0, 0) (0, 0)
(0, 0) (0, 0) (0, 0) (0, 0)
(0, 0) (0, 0) (0, 0) (-1, 0)

90pulse + delay 100 + 180pulse

after multiple pulses:

(-0.000511, 0) (0.543, -0.0246) (0.452, 0.00457) (2.96e-005,1.32e-005)
(0.543, 0.0246) (-0.000549, 0) (7.31e-005,-0.000133) (0.543, 0.0242)
(0.452, -0.00457) (7.31e-005, 0.000133) (0.00049, 0) (0.452, -0.00487)
(2.96e-005,-1.32e-005) (0.543, -0.0242) (0.452, 0.00487) (0.00057, 0)

t90 = 1.6666666666666667

Saved files: multiple2_11.spe

J=50 Hz; v1=0 Hz, v2=80 Hz

start matrix:

(1, 0) (0, 0) (0, 0) (0, 0)
(0, 0) (0, 0) (0, 0) (0, 0)
(0, 0) (0, 0) (0, 0) (0, 0)
(0, 0) (0, 0) (0, 0) (-1, 0)

90pulse + delay 100 + 180pulse

after multiple pulses:

(-0.000448, 0) (0.535, -0.0183) (0.462, 0.00532) (1.97e-005,6.86e-006)

(0.535, 0.0183) (-0.000468, 0) (5.24e-005,-0.000126) (0.535, 0.018)
(0.462, -0.00532) (5.24e-005, 0.000126) (0.000428, 0) (0.462, -0.00557)
(1.97e-005,-6.86e-006) (0.535, -0.018) (0.462, 0.00557) (0.000488, 0)
t90 = 1.6666666666666667
Saved files: multiple2_12.spe

J=50 Hz; v1=0 Hz, v2=50 Hz

start matrix:
(1, 0) (0, 0) (0, 0) (0, 0)
(0, 0) (0, 0) (0, 0) (0, 0)
(0, 0) (0, 0) (0, 0) (0, 0)
(0, 0) (0, 0) (0, 0) (-1, 0)
90pulse + delay 100 + 180pulse
after multiple pulses:
(-0.000309, 0) (0.523, -0.0101) (0.476, 0.00489) (8e-006, 1.7e-006)
(0.523, 0.0101) (-0.00031, 0) (2.29e-005,-9.33e-005) (0.523, 0.00988)
(0.476, -0.00489) (2.29e-005,9.33e-005) (0.000294, 0) (0.476, -0.00505)
(8e-006,-1.7e-006) (0.523, -0.00988) (0.476, 0.00505) (0.000325, 0)
t90 = 1.6666666666666667
Saved files: multiple2_13.spe

J=50 Hz; v1=0 Hz, v2=20 Hz

start matrix:
(1, 0) (0, 0) (0, 0) (0, 0)
(0, 0) (0, 0) (0, 0) (0, 0)
(0, 0) (0, 0) (0, 0) (0, 0)
(0, 0) (0, 0) (0, 0) (-1, 0)
90pulse + delay 100 + 180pulse
after multiple pulses:
(-0.000131, 0) (0.509, -0.00344) (0.491, 0.00257) (1.31e-006, 1.1e-007)
(0.509, 0.00344) (-0.000127, 0) (3.89e-006,-4.06e-005) (0.509, 0.00338)
(0.491, -0.00257) (3.89e-006,4.06e-005) (0.000125, 0) (0.491, -0.00264)
(1.31e-006,-1.1e-007) (0.509, -0.00338) (0.491, 0.00264) (0.000134, 0)
t90 = 1.6666666666666667
Saved files: multiple2_15.spe

J=50 Hz; v1=0 Hz, v2=10 Hz

start matrix:

(1, 0) (0, 0) (0, 0) (0, 0)

(0, 0) (0, 0) (0, 0) (0, 0)

(0, 0) (0, 0) (0, 0) (0, 0)

(0, 0) (0, 0) (0, 0) (-1, 0)

90pulse + delay 100 + 180pulse

after multiple pulses:

(-4.25e-015, 0) (0.5,-3.68e-016) (0.5,-4.02e-016) (-9.99e-016,1.73e-016)

(0.5,3.68e-016) (1.05e-015, 0) (1.14e-015,-4.16e-017) (0.5,-4.37e-016)

(0.5,4.02e-016) (1.14e-015,4.16e-017) (1.22e-015, 0) (0.5,-4.16e-016)

(-9.99e-016,-1.73e-016) (0.5,4.37e-016) (0.5,4.16e-016) (2.22e-015, 0)

t90 = 1.6666666666666667

Saved files: multiple2_16.spe

2.3 Density matrices for different scalar couplings

J=0 Hz; v1=0 Hz, v2=100 Hz

start matrix:

(1, 0) (0, 0) (0, 0) (0, 0)

(0, 0) (0, 0) (0, 0) (0, 0)

(0, 0) (0, 0) (0, 0) (0, 0)

(0, 0) (0, 0) (0, 0) (-1, 0)

90pulse + delay 100 + 180pulse

after multiple pulses:

(-0.000539, 0) (0.5,-1.44e-017) (0.5,-0.000334) (1.33e-015,-5.6e-016)

(0.5,1.44e-017) (-0.000539, 0) (-1.25e-015,-4.33e-016) (0.5,-0.000334)

(0.5, 0.000334) (-1.25e-015,4.33e-016) (0.000539, 0) (0.5,9.72e-016)

(1.33e-015, 5.6e-016) (0.5, 0.000334) (0.5,-9.72e-016) (0.000539, 0)

t90 = 1.6666666666666667

Saved files: multiple3_9.spe

J=10 Hz; v1=0 Hz, v2=100 Hz

start matrix:

(1, 0) (0, 0) (0, 0) (0, 0)

(0, 0) (0, 0) (0, 0) (0, 0)

(0, 0) (0, 0) (0, 0) (0, 0)

(0, 0) (0, 0) (0, 0) (-1, 0)

90pulse + delay 100 + 180pulse

after multiple pulses:

(-0.000533, 0) (0.509, -0.00264) (0.49, -0.00176) (5.97e-006,2.66e-006)
(0.509, 0.00264) (-0.000544, 0) (1.47e-005,-2.68e-005) (0.509, 0.0023)
(0.49, 0.00176) (1.47e-005,2.68e-005) (0.000532, 0) (0.49, 0.00144)
(5.97e-006,-2.66e-006) (0.509, -0.0023) (0.49, -0.00144) (0.000545, 0)
t90 = 1.6666666666666667
Saved files: multiple3_10.spe

J=20 Hz; v1=0 Hz, v2=100 Hz

start matrix:

(1, 0) (0, 0) (0, 0) (0, 0)
(0, 0) (0, 0) (0, 0) (0, 0)
(0, 0) (0, 0) (0, 0) (0, 0)
(0, 0) (0, 0) (0, 0) (-1, 0)

90pulse + delay 100 + 180pulse

after multiple pulses:

(-0.000527, 0) (0.519, -0.00647) (0.481, -0.00198) (1.19e-005,5.32e-006)
(0.519, 0.00647) (-0.000548, 0) (2.94e-005,-5.36e-005) (0.519, 0.00612)
(0.481, 0.00198) (2.94e-005,5.36e-005) (0.000524, 0) (0.481, 0.00166)
(1.19e-005,-5.32e-006) (0.519, -0.00612) (0.481, -0.00166) (0.000551, 0)
t90 = 1.6666666666666667
Saved files: multiple3_11.spe

J=50 Hz; v1=0 Hz, v2=100 Hz

start matrix:

(1, 0) (0, 0) (0, 0) (0, 0)
(0, 0) (0, 0) (0, 0) (0, 0)
(0, 0) (0, 0) (0, 0) (0, 0)
(0, 0) (0, 0) (0, 0) (-1, 0)

90pulse + delay 100 + 180pulse

after multiple pulses:

(-0.000486, 0) (0.566, -0.0724) (0.416, 0.0367) (5.78e-005,2.58e-005)
(0.566, 0.0724) (-0.00052, 0) (0.000144,-0.000257) (0.566, 0.072)
(0.416, -0.0367) (0.000144, 0.000257) (0.000404, 0) (0.416, -0.0369)
(5.78e-005,-2.58e-005) (0.566, -0.072) (0.416, 0.0369) (0.000602, 0)
t90 = 1.6666666666666667
Saved files: multiple3_13.spe

J=100 Hz; v1=0 Hz, v2=100 Hz

start matrix:

(1, 0) (0, 0) (0, 0) (0, 0)
(0, 0) (0, 0) (0, 0) (0, 0)
(0, 0) (0, 0) (0, 0) (0, 0)
(0, 0) (0, 0) (0, 0) (-1, 0)

90pulse + delay 100 + 180pulse

after multiple pulses:

(-0.000454, 0) (0.522, -0.181) (0.419, 0.138) (0.000104,4.72e-005)
(0.522, 0.181) (-0.000347, 0) (0.00027, -0.00044) (0.522, 0.181)
(0.419, -0.138) (0.00027, 0.00044) (0.000138, 0) (0.419, -0.138)
(0.000104,-4.72e-005) (0.522, -0.181) (0.419, 0.138) (0.000663, 0)

t90 = 1.6666666666666667

Saved files: multiple3_15.spe

J=500 Hz; v1=0 Hz, v2=100 Hz

start matrix:

(1, 0) (0, 0) (0, 0) (0, 0)
(0, 0) (0, 0) (0, 0) (0, 0)
(0, 0) (0, 0) (0, 0) (0, 0)
(0, 0) (0, 0) (0, 0) (-1, 0)

90pulse + delay 100 + 180pulse

after multiple pulses:

(-0.000504, 0) (0.269, 0.0318) (0.653, 0.0294) (0.000118,6.02e-005)
(0.269, -0.0318) (0.000406, 0) (0.00036,1.89e-005) (0.269, -0.032)
(0.653, -0.0294) (0.00036,-1.89e-005) (-0.000641, 0) (0.653, -0.0298)
(0.000118,-6.02e-005) (0.269, 0.032) (0.653, 0.0298) (0.000739, 0)

t90 = 1.6666666666666667

Saved files: multiple3_14.spe